Title

Stimulation of isoprene emissions and electron transport rates as key mechanisms of thermal tolerance in the tropical species Vismia guianensis

Journal

Global Change Biology, 26(10)

ISSN

1354-1013

Authors

Rodrigues, Tayana B
Baker, Christopher R
Walker, Anthony P
et al.

Publication Date

2020-10-01

DOI

10.1111/gcb.15213

Peer reviewed

Stimulation of isoprene emissions and electron transport rates are a key mechanism of thermal tolerance in the tropical species *Vismia guianensis*

Running Title: Temperature, isoprene, and photochemistry

Tayana B. Rodrigues[1], Christopher R. Baker[2], Anthony P. Walker[3], Nate McDowell[4], Alistair Rogers[5], Niro Higuchi[1], Jeffrey Q. Chambers[1,6], Kolby J. Jardine*[1,6]

[1.] *Forest Management Laboratory, National Institute of Amazonian Research, Manaus, Amazonas, Brazil*
[2.] *Howard Hughes Medical Institute, Department of Plant and Microbial Biology, University of California, Berkeley, CA, USA*
[3.] *Environmental Sciences Division and Climate Change Science Institute, Oak Ridge National Laboratory, Oak Ridge, TN, USA*
[4.] *Earth System Analysis and Modeling, Pacific Northwest National Laboratory, Richland, WA, USA*
[5.] *Environmental and Climate Sciences Department, Brookhaven National Laboratory, Upton, NY, USA*
[6.] *Climate and Ecosystem Sciences Division, Lawrence Berkeley National Laboratory, Berkeley, CA, USA*
*Author for correspondence:
Kolby Jardine
Tel: (510) 495-8231
Email: kjjardine@lbl.gov

Total word count (excluding summary, references and legends):	6,661	N° of figures:	6 (all in color)
Summary:	285	N° of tables:	1
Introduction:	2,036		
Material and Methods:	1,548		
Results:	1,038		
Discussion:	1,934		
Acknowledgements	105		

Summary

Tropical forests absorb large amounts of atmospheric CO_2 through photosynthesis, but high surface temperatures suppress this absorption while promoting isoprene emissions. While mechanistic isoprene emission models predict a tight coupling to photosynthetic electron transport (ETR) as a function of temperature, direct field observations of these phenomenon are lacking in the tropics and are necessary to assess the impact of a warming climate on global isoprene emissions. Here, we demonstrate that in the early successional species *Vismia guianensis* in the central Amazon, ETR rates increased with temperature in concert with isoprene emissions, even as stomatal conductance (g_s) and net photosynthetic carbon fixation (P_n) declined. We observed the highest temperatures of continually increasing isoprene emissions yet reported (50°C). While P_n showed an optimum value of 32.6 ± 0.4°C, isoprene emissions, ETR, and the oxidation state of PSII reaction centers (q_L) increased with leaf temperature with strong linear correlations for ETR (p = 0.98) and q_L (p = 0.99) with leaf isoprene emissions. In contrast, other photoprotective mechanisms, such as non-photochemical quenching (NPQ), were not activated at elevated temperatures. Inhibition of isoprenoid biosynthesis repressed P_n at high temperatures through a mechanism that was independent of stomatal closure. While extreme warming will decrease g_s and P_n in tropical species, our observations support a thermal tolerance mechanism where the maintenance of high photosynthetic capacity under extreme warming is assisted by the simultaneous stimulation of ETR and metabolic pathways that consume the direct products of ETR including photorespiration and the biosynthesis of thermoprotective isoprenoids. Our results confirm that models which link isoprene emissions to the rate of ETR hold true in tropical species and provide necessary "ground-truthing" for simulations of the large predicted increases in tropical isoprene emissions with climate warming.

Key words: *global warming, high temperature stress, leaf gas exchange, chlorophyll fluorescence, fosmidomycin, electron transport rates, net photosynthesis, isoprene energetic requirements*

1. Introduction

Tropical forests absorb large amounts of atmospheric CO_2, accounting for an estimated ~34% (42 Pg C yr^{-1}) of global terrestrial gross primary production (Beer *et al.*, 2010). However, substantial decreases in tropical forest gross primary productivity have been repeatedly demonstrated in the Amazon basin during periodic widespread drought associated with high temperature (Potter *et al*. 2011; Liu *et al.*, 2017). Therefore, the physiological mechanisms through which tropical forests respond to high temperature are critically important to understand. One such mechanism is the biosynthesis and emission of the volatile organic compound isoprene (C_5H_8), which can act as a thermotolerant and may be associated with stress protection at elevated temperatures (Jardine *et al*. 2017, Sharkey and Yeh 2001).

During photosynthesis, energy from absorbed light is dissipated by three processes: photochemistry, chlorophyll fluorescence, and thermal dissipation (measured as non-photochemical quenching, NPQ). The relative contribution of these three processes to total energy dissipation is highly sensitive to leaf temperature (Müller *et al.*, 2001). Chlorophyll fluorescence is light emitted at wavelengths centered on 682 nm or 740 nm (Krause & Weis, 1984) and changes in fluorescence and derived photochemical parameters during high leaf temperatures have been widely used to provide insight into photochemical metabolism (Li *et al.*, 2009). For example, variable chlorophyll fluorescence (Fv), is the difference between the maximum (Fm) and minimum fluorescence (Fo). Decreases in the ratio (Fv/Fm) of variable (Fv) to maximum (Fm) chlorophyll fluorescence have been widely used to demonstrate environmental stress effects on the quantum

efficiency of Photosystem II (Murchie and Lawson 2013). During the 2015/2016 El Niño Amazon drought, sun-induced fluorescence, a metric of gross primary productivity, was strongly suppressed over areas with anomalously high temperatures and decreased levels of soil moisture (Koren *et al.*, 2018). Elevated leaf temperatures strongly enhance leaf-to-atmosphere vapor pressure deficits which drives high leaf transpiration rates and reductions in plant water potentials. To avoid excessive water loss and hydraulic failure, an afternoon reduction in stomatal conductance (g_s) is often observed, resulting in an afternoon depression of P_n during warm afternoons (Koch *et al.*, 1994; Chambers & Silver, 2004). In the Tapajos National Forest in east-central Amazon, a corresponding mid-day and post mid-day depression in net ecosystem exchange of CO_2 was regularly observed using eddy covariance (Piedade *et al*., 1994; Goulden *et al*., 2004).

It has been hypothesized that reductions in P_n at high leaf temperatures in tropical species, are mainly associated with reductions in g_s rather than direct negative temperature effects on photosynthetic electron transport, or the light-independent reactions of photosynthesis (Lloyd & Farquhar, 2008). However, few experimental observations in the tropics have evaluated these hypotheses, especially in early successional species that tend to show high rates of P_n. The Neotropical early successional genera *Vismia* dominates large rainforest disturbance gaps in the Amazon Basin (Chambers *et al*., 2009) where it helps accelerate the regeneration of secondary forests by influencing forest successional pathways (Uhl *et al*., 1988; Zalamea & González, 2008; Brienen *et al*., 2015). The establishment of early successional genera in secondary forests is related to their ability to maintain high P_n and growth under conditions of full sunlight and high leaf temperatures characteristic of tropical landscapes impacted by natural (Chambers *et al*., 2009) and human (Mesquita *et al*., 2015) disturbances. *Vismia* leaves show high rates of isoprene emissions (Jardine *et al*., 2016), which is hypothesized to play an important role in thermotolerance of

98 photosynthesis (Singsaas *et al*., 1997; Sharkey *et al.*, 2001; Sharkey, 2005; Sasaki *et al*., 2007). As
99 previously reviewed (Harley *et al.*, 1999), stimulation of isoprene production by high irradiance
100 and warm temperatures is consistent with physiological evidence of a role in ameliorating stresses
101 associated with warm and high-light environments.

102 Plants utilize the products of both the light (ATP and NADPH) and light-independent
103 reactions of photosynthesis to synthesize a number of photosynthetic components and defense
104 compounds via the isoprenoid pathway in chloroplasts (Lichtenthaler, 1987; Affek & Yakir, 2003).
105 Tropical ecosystems are recognized as the largest source of isoprene emissions to the atmosphere,
106 representing roughly half of the estimated global annual emissions of 440-660 Tg C yr^{-1} (Guenther
107 *et al.*, 2006). Isoprene biosynthesis begins with the initial condensation of pyruvate and
108 glyceraldehyde-3-phosphate derived from the Calvin-Benson-Bassham cycle (Silver & Fall,
109 1995). Leaf isoprene emissions are strongly stimulated by temperature (Duncan *et al.*, 2009) with
110 global emission models predicting future increases in tropical forest isoprene emissions and their
111 corresponding impacts on atmospheric chemistry and climate including altering the dynamics and
112 lifetimes of atmospheric oxidants, secondary organic aerosols, and cloud condensation nuclei
113 (Pacifico *et al.*, 2009). Isoprene emissions from terrestrial plants are completely dependent on
114 illumination (Sanadze, 1991), including tropical trees (Jardine *et al.*, 2014), consistent with the
115 view that the isoprenoid pathway is completely dependent on photosynthetic electron transport
116 (Lantz *et al.*, 2019).

117 While the mechanisms of isoprene thermotolerance are under investigation, recent
118 literature suggests that isoprene and other isoprenoids protect photosynthesis during abiotic stress
119 by minimizing oxidative damage through a number of mechanisms including; physical
120 stabilization of photosynthetic membranes, the consumption of photosynthetic energy and

reducing equivalents, direct antioxidant reactions (e.g. between isoprene and reactive oxygen species including fatty acid peroxyl radicals), and potent phytohormone signaling properties of isoprene including oxidation products methyl vinyl ketone and methacrolein which activate defense gene expression (Singsaas *et al.*, 1997; Velikova *et al.*, 2008; Vickers *et al.*, 2009a, 2009b; Karl *et al.*, 2010; Jardine *et al.*, 2012; Morfopoulos *et al.*, 2014, Junker-Frohn *et al*., 2019, Zuo *et al.,* 2019). For example, in *Populus nigra* and *Phragmites australis* leaves exposed to oxidative stress, reduced damage to photosynthesis, accumulation of H_2O_2, and membrane denaturation was attributed, in part, to isoprene production (Velikova *et al.*, 2008). However, there is limited evidence for the occurrence of these mechanisms in the tropics where field data are scarce.

Leaf isoprene emissions are generally assumed to account for 1–2% of P_n at leaf temperatures below the optimum for P_n, but have been reported to represent 10% of P_n or higher at temperatures above the optimum (Harley *et al.*, 1996). While P_n in tropical trees generally have an optimum leaf temperature between 28 - 32°C, emissions of isoprene at the leaf level have been consistently shown to continue to increase up to 40°C or beyond (Alves *et al.,* 2014; Jardine *et al.,* 2014, 2017a). Observations at ecosystem scales in the tropics observed the highest isoprenoid emission fluxes during the hottest period of the day (12:00h–14:00h) when g_s and P_n are reduced (Karl *et al.,* 2009; Jardine *et al.,* 2011, 2017a). Therefore, the increasing importance of isoprene emissions to plant carbon budgets under high temperatures is recognized as a consequence of both the stimulation of isoprene emissions and the suppression of P_n (Monson *et al.*, 1992). $^{13}CO_2$ labeling revealed that under optimal conditions of P_n, 70 - 90% of the carbon used for isoprene synthesis is produced from recently assimilated atmospheric CO_2 (Delwiche & Sharkey, 1993; Affek & Yakir, 2003). In contrast, under high leaf temperatures and drought conditions where P_n is suppressed, isoprene carbon sources have been shown to increasingly derive from previously

assimilated or stored carbon (Funk *et al*., 2004). While a number of extrachloroplastic metabolites have been considered as 'alternate' carbon including pyruvate, glucose, acetate, and the C_1 pathway (Jardine *et al.*, 2010, 2017b; Kreuzwieser *et al.*, 2002, de Souza *et al*., 2018), evidence using ^{13}C-labeled photorespiratory intermediates and CO_2-free atmospheres suggest that re-assimilation of internal plant sources of CO_2 like photorespiration, respiration, and xylem-transported CO_2 may help explain this 'alternate' carbon source for isoprene and contribute to the suppression of P_n at high temperatures (Jardine *et al*., 2014, 2017a; Garcia *et al*., 2019; Guidolotti *et al.,* 2019). This is consistent with the recent observation that the majority of xylem-transported CO_2 is re-assimilated in illuminated leaves (Stutz & Hanson, 2019).

In addition to strong uncoupling between isoprene emissions and P_n at high temperature, elevated CO_2 has been widely reported to stimulate P_n while suppressing isoprene emissions (Loreto & Sharkey, 1993). While various mechanisms including a key role of extrachloroplastic intermediates have been discussed in the literature, recent evidence suggests that the elevated CO_2 effect is largely driven by a limited supply of energetic and reductive equivalents for isoprenoid biosynthesis generated by the photochemical phase of photosynthesis (Rasulov *et al.*, 2009, 2018; Morfopoulos *et al.*, 2014). In 2002, strong positive correlations was first described between foliage isoprenoid emissions and photosynthetic electron transport rates (ETR) in the Mediterranean trees *Quercus coccifera* and *Q. ilex* (Niinemets *et al.*, 2002a) and an early model was developed discussing light-dependent NADPH limitation of isoprenoid leaf emissions (Niinemets *et al.*, 2002b). Following these initial discoveries and developments, positive linear correlation between ETR and isoprene emissions were observed at elevated CO_2 mixing ratios in both *Quercus pubescens* and *Quercus ilex* (Rapparini *et al.*, 2004), and later a model was developed showing NADPH limitation of isoprene emissions under different light, leaf intercellular CO_2

concentrations (C_i) and temperature conditions (Morfopoulos *et al.*, 2013). A similar model was then used to explain how the elevated CO_2 enhancement of P_n, but suppression of isoprene emission, is driven by a limited supply of NADPH for isoprenoid biosynthesis (Morfopoulos *et al.*, 2014), and these mechanisms were extended to include drought effects where increased isoprene emissions are maintained due to the increased ratio of ETR to P_n. (Dani *et al.*, 2015).

Using post-illumination isoprene bursts to estimate the pool size of the isoprene precursor dimethylallyl diphosphate (DMADP) in oak (*Quercus robur*) and poplar (*Populus deltoides*) leaves, DMADP was observed to increase with temperature up to 35°C (Li *et al.*, 2011). ETRs in many plants generally demonstrate higher optimum leaf temperatures than P_n under current atmospheric CO_2 concentrations (Ishida & Toma, 1999; Himalayan & Tech, 2005; Sage & Kubien, 2007) and isoprene energetic models predict a temperature optimum of isoprene emissions that closely follows the temperature optimum of ETR (a temperature optimum higher than P_n but lower than that of isoprene synthase activity) (Morfopoulos *et al.*, 2013). Thus, there is considerable evidence that the rate-limiting steps for isoprenoid biosynthesis *in vivo* depends on the availability of NADPH and ATP in the chloroplast, the direct products of ETR (Rasulov *et al*., 2009, 2018). Unfortunately, studies with parallel measurements of ETR and isoprene emissions as a function of temperature are relatively rare and experimental data on abundant tropical species at high temperature is lacking.

Here we hypothesize that in early successional tropical species high temperatures will be associated with an enhanced rate of production of the energetic and reductive equivalents necessary for isoprenoid biosynthesis and generated by the photochemical phase of photosynthesis. Thus, in spite of reduced P_n at high temperatures, ETR will continue to increase at elevated temperatures together with high isoprenoid biosynthesis rates and other chloroplastic

NADPH/ATP consuming pathways such as photorespiration (Voss *et al.*, 2013), thereby limiting rates of NPQ at high temperatures. We also hypothesize that inhibition of isoprenoid biosynthesis would reduce P_n at high temperatures both due to the direct loss of the thermoprotective role of isoprene as well as the potential antioxidant and signaling roles of isoprene. We test these hypotheses by quantifying the suppression of P_n and g_s at high leaf temperatures together with changes in photochemical parameters of photosynthesis and isoprene emissions in the fast growing early successional species *Vismia guianensis* (Aubl.) Pers in the central Amazon. We combine gas exchange during leaf temperature response curves with chlorophyll fluorescence and isoprene emissions, and therefore simultaneously characterize the temperature sensitivities of P_n, g_s, isoprene emissions, and key parameters of the photochemical reactions of photosynthesis including ETR, non-photochemical quenching (NPQ), the oxidation state of PSII reaction centers (q_L), and the maximum quantum efficiency of PSII in the dark (Fv/Fm) and light (Fv'/Fm').

Further, by delivering a specific inhibitor of the isoprenoid pathway (fosmidomycin) to detached *V. guianensis* branches, we evaluate the impact of blocking isoprenoid production on P_n at high leaf temperatures. We discuss the results in terms of thermotolerance mechanisms in tropical plants including the role of isoprene may have in supporting the upregulation of ETR rather than NPQ at high leaf temperatures. Finally, we discuss the implications for modeling of future isoprene emissions from tropical forests and interpretation of remote sensing studies tracking seasonal patterns in regional isoprene emissions, gross primary productivity, and canopy temperature.

2. Materials and Methods

2.1 Site description

Coupled gas-exchange and chlorophyll fluorescence measurements were carried out on three individuals of *V. guianensis* (Aubl.) Pers., an early successional tree species from the Hypericaceae family. Four *V. guianensis* individuals were studied in the Reserva Biológica do Cuieiras (ZF2), a primary rainforest biological reserve located approximately 60 km northwest of Manaus, in the central Amazon Basin, Brazil (Higuchi *et al.*, 1998). The *V. guianensis* individuals ranged between 1.6 m and 2.0 m in height and were exposed to full sunlight conditions throughout a large part of the day due to their presence in gap associated with the site access road.

2.2 Gas exchange data

The coupled leaf isoprene emissions, gas exchange, and chlorophyll fluorescence field measurements were made during October 2017 and April, May, June, July, and August of 2018. For each of the four *V. guianensis* individuals, 2-8 leaf temperature response curves were conducted between 7:00-15:00 (23 total response curves, 1-3 per day). All leaves selected for study were dark green and considered developmentally and physiologically mature, with no obvious visual problems and little herbivory. Previous research has shown that mature *V. guianensis* leaves in the central Amazon showed substantially higher rates of P_n, isoprene emissions, and g_s under standard environmental conditions than young, rapidly expanding light green leaves (Jardine *et al*., 2016).

Gas exchange responses to leaf temperature for *V. guianensis* leaves were collected in the field using a portable photosynthesis system with a 2 cm^2 leaf fluorescence chamber (6400XT, Licor Biosciences) adapted for the collection of isoprene emissions by the diversion of a fraction (100 ml min^{-1}) of the air sample leaving the leaf chamber through a clean thermal desorption tube packed with Quartzwool, Tenax TA and Carbograph 5TD adsorbents (Markes International) for 10 min using a hand-held pump (APEX, Casella, USA) (Jardine *et al.*, 2015b). Each leaf placed in

the chamber was maintained under constant photosynthetically active radiation (PAR) of 0 μmol m^{-2} s^{-1} for the dark temperature response curve. In a previous study at constant leaf temperature (30°C) we showed that during both the wet and dry seasons, developmentally and physiologically mature *V. guianensis* leaves reached light saturation of P_n at PAR fluxes between 750-1000 μmol m^{-2} s^{-1} (Jardine *et al*., 2016). Thus, we chose to conduct all leaf temperature response curves in the wet and dry seasons under the standard PAR flux of 1000 μmol m^{-2} s^{-1}, which also facilitates future modeling studies requiring the standard isoprene emission potential parameter, defined as the emissions under 30°C and 1000 μmol m^{-2} s^{-1} PAR. Throughout temperature response curves in the dark and light, the reference CO_2 concentration was maintained at 400 ppm, and air flow rate entering the leaf chamber was held constant at 400 μmol s^{-1}. Once the leaf was placed in the chamber at 0 μmol m^{-2} s^{-1} PAR, a black cloth was used to cover the chamber. Following a 15 min period of leaf dark adaption, the dark leaf temperature response curve was initiated to demonstrate the lack of isoprene emissions in the dark and to acquire the dark parameters of chlorophyll fluorescence. Following the completion of the dark temperature response curve, the black cloth was removed, the PAR was set at 1000 μmol m^{-2} s^{-1}. Following a period of light adaptation required to reach steady state gas exchange (10-40 min), the temperature response curve of the illuminated leaf was initiated. Leaf temperature response curves were generated by setting the block temperature to 25, 27.5, 30.0, 32.5, 35, 37.5, 40, and 42.5 ºC, sequentially. The leaf temperature was directly measured using a leaf thermocouple mounted inside the leaf chamber.

2.3 Chlorophyll Fluorescence

For all leaves studied during October 2017 and April, May, June, July, and August of 2018, a leaf chamber fluorimeter (LCF 6400-40, Licor Biosciences) was used to simultaneously quantify leaf gas exchange and chlorophyll fluorescence. The fluorimeter was unavailable during the

isoprenoid inhibition experiments which occurred earlier during the July 2017 (see **section 2.5**). Following leaf acclimation to each successive temperature increase, an actinic light pulse of 7,000 μmol m^{-2} s^{-1} (10% blue light and 90% red light), modulated at 20 KHz, was applied for 1 sec and the average chlorophyll fluorescence signal was recorded. The average chlorophyll fluorescence signal at each leaf temperature was used to determine minimum fluorescence (Fo), maximum fluorescence (Fm), and steady-state fluorescence (Fs). Derived photochemical parameters at each leaf temperature were calculated according to **Eqs. 1-5** where derived parameters with prime, for example Fo`, are values related to the data in the light and those with no prime corresponding to data from the dark adapted leaf (Baker & Rosenqvist, 2004).

The electron transport rate (ETR, μmol e^- m^{-2} s^{-1}) was calculated according to **Eq. 1**, where f is the fraction of the quantum absorbed and used by Photosystem II, with a value of 0.5 used for C_3 plants (Earl & Tollenaar, 1998), PAR is incident photon flux density, and α_{leaf} is leaf absorbance (0.87).

Eq. 1. $$ETR = \left(\frac{Fm` - Fs}{Fm`}\right) f \cdot PAR \cdot \alpha_{leaf}$$

The redox state of Q_A, the primary electron accepter of PSII, was determined by quantification of the photochemical extinction coefficient (q_L) according to **Eq. 2**. q_L is an estimate of the average oxidation level of PSII reaction centers. which is a measure of the fraction of Q_A in an oxidized state (Kramer & Johnson, 2004). Thus, an increase in q_L indicates that average oxidation level of PSII increased to support, for example, an upregulation of ETR, NADPH/ATP production, and isoprenoid biosynthesis.

Eq. 2. $$qL = \frac{\frac{1}{Fs} - \frac{1}{Fm'}}{\frac{1}{Fo'} - \frac{1}{Fm'}}$$

Photon capture efficiency of photosynthetic reaction centers in the light was estimated according to **Eq. 3**.

Eq. 3. Maximum quantum efficiency of PSII photochemistry of dark adapted leaves: $\frac{Fv}{Fm}$, and light adapted leaves: $\frac{Fv'}{Fm'}$

Finally, we estimated non-photochemical quenching (NPQ) according to **Eq. 4**.

Eq. 4. $NPQ = \frac{Fm - Fm`}{Fm`}$

Immediately following the chlorophyll fluorescence measurements, isoprene emissions were collected on a single thermal desorption tube for 10 minutes while gas exchange data were logged simultaneously on the Li6400XT.

2.4 Leaf isoprene emissions

Following sample collection in the field, the thermal desorption tubes were transported to the laboratory in Manaus, Brazil, for the analysis of adsorbed isoprene using an automated thermal desorption system (TD-100, Thermal Desorber, Markes International, UK) coupled to a gas chromatograph (series 7890A, Agilent Technologies, USA) and mass spectrometer (Agilent ChemStation, Agilent Technologies, USA) (TD-GC-MS) installed at the National Research Institute of the Amazon (INPA) (Jardine *et al.*, 2015a). The system was calibrated for isoprene using m/z 67 as the most abundant ion formed during electron impact ionization as previously described (Jardine *et al.*, 2016). The average leaf isoprene emission rate (nmol m^{-2} s^{-1}) at each leaf temperature was calculated according to **Eq. 6** where PA67 is the GC-MS peak area at the retention time for isoprene (ion counts of m/z 67 x min), Cal is the calibration factor determined for isoprene (10^{-6} nL isoprene/peak area), F is the flow rate of air into the leaf chamber (400 µmol s^{-1}), 10^{-6} is the factor used to convert µmoles to moles, $Leaf_{Area}$ is the leaf area enclosed in the chamber of 0.0002 m^2, and Volume is the total volume of air that passed through the thermal desorption tube (1.0 L).

306 **Eq. 6**. $Isoprene\ emission = PA67 \times Cal \times F \times 10^{-6}/(Leaf_{Area} * Volume)$

307

308 **2.5 Inhibition of the isoprenoid pathway with fosmidomycin**

309 In a separate experiment during July and August of 2017, we inhibited the production of
310 leaf isoprene in *V. guianensis*, by feeding excised branches with 12.5 mM fosmidomycin. Branches
311 were cut between 8:00h-8:30h and then immediately recut under either water (control, 4 branches,
312 1 branch per individual) or the fosmidomycin solution (3 branches, 1 branch per individual) and
313 allowed to transpire for 1h in full sunlight in order to ensure delivery of the inhibitor to the leaves.
314 Previous work has shown that a low concentration of fosmidomycin (4 μM) delivered to leaves of
315 mid-latitude species was sufficient to inhibit leaf isoprene emissions (Sharkey & Yeh, 2001).
316 However, in our study we found that 12.5 mM fosmidomycin solution was required to completely
317 inhibit production of leaf isoprene in *V. guianensis*. Following inhibitor uptake, the temperature
318 response curves of gas exchange and isoprene emissions were measured as described above with
319 the exception that we used the standard 6 cm^2 leaf chamber with red and blue LED light source
320 (6400-02B, Licor Biosciences, USA). Note that in the inhibitor experiments with detached
321 branches, we were able to achieve higher leaf temperatures due to direct solar heating of the
322 chamber because of cloud free conditions during the 2017 dry season.

323 **2.6 Statistical Analysis**

324 Statistical analysis of the 23 leaf temperature response curves included calculating the mean
325 and confidence interval (± 2 standard deviation) of the leaf temperature, gas exchange
326 characteristics (e.g. P_n and g_s), photochemical characteristics (e.g. ETR, qL, Fv'/Fm', and NPQ),
327 and isoprene emissions at each block temperature. Pearson product-moment correlation
328 coefficients were determined between each possible pair of mean gas exchange and photochemical
329 variables together with mean isoprene emissions (**Table 1**). Linear coefficients of determination

(R^2) and the equations were determined during regression analysis between isoprene emissions and the photochemical parameters ETR and q_L.

For the isoprenoid inhibitor experiments where gas exchange and isoprene emissions were collected from 4 water-fed control branches and 3 inhibitor-fed branches, the mean and confidence interval (± 2 standard deviation) calculations were made as a function of leaf temperature for P_n, g_s, C_i, and isoprene emissions.

3. Results

3.1 Gas exchange and photochemical parameters

Figures 1-2 show mean (± 2 standard deviations) gas exchange and photochemical parameters as a function of mean leaf temperature. As leaf temperature increased from the lowest value of 26.7 ± 0.5°C to 32.6 ± 0.4°C, net photosynthesis (P_n) and transpiration (E) were stimulated to maximum values of 10.2 ± 1.1 μmol m^{-2} s^{-1} and 3.9 +/- 0.5 mmol m^{-2} s^{-1}, respectively. As leaf temperatures continued to increase from 32.6 ± 0.4 °C to the highest value (38.3 ± 0.4°C), P_n decreased by 16% and reached a minimum of 8.6 ± 1.9 μmol m^{-2} s^{-1}, while E decreased by 21% to 3.1 +/- 0.9 mmol m^{-2} s^{-1}. In contrast, g_s continuously decreased as leaf temperature increased. At the lowest leaf temperature of 26.7 ± 0.5°C, g_s was at a maximum value of 0.21 ± 0.05 mol m^{-2} s^{-1}, while at 38.3 ± 0.4°C, g_s reached a minimum value of 0.09 ± 0.04 mmol m^{-2} s^{-1}, representing a 57% decline. Similarly, intracellular CO_2 (C_i) levels decreased linearly with leaf temperature, which is consistent with the decline in P_n being driven by the reduction in g_s as opposed to a decline in photosynthetic capacity (**Fig. 1**).

Together with isoprene emissions, two of the photochemical parameters (ETR and q_L) associated with the light reactions of photosynthesis (**Fig. 2**) were strongly stimulated by increasing temperatures with no sign of saturation or decline. A minimum ETR value of 123.1 ±

354 24.5 μmol e^- m^{-2} s^{-1} occurred at the lowest leaf temperature (26.7 ± 0.5°C) and continuously
355 increased with leaf temperature to reach a maximum value of 189.4 ± 34.2 μmol e^- m^{-2} s^{-1} at the
356 highest leaf temperature (38.3 ± 0.4°C), representing a 54% increase. Similarly, over the same
357 temperature range, q_L increased by 39% from 0.39 ± 0.06 at the lowest leaf temperature to 0.54 ±
358 0.05 at the highest leaf temperature, demonstrating that the average oxidation level of PSII
359 increased consistently as leaf temperature increased. Together with these photochemical
360 parameters, leaf isoprene emissions were strongly stimulated by increases in leaf temperature by
361 490% over the temperature range studied. Isoprene emissions were at a minimum of 6.1 ± 1.9 nmol
362 $m^{-2}s^{-1}$ at the lowest leaf temperature and increased to maximum emission rate of 29.9 ± 3.8 nmol
363 $m^{-2}s^{-1}$ at the highest leaf temperature. In contrast, NPQ was variable and did not show any clear
364 trend with leaf temperature; NPQ was 1.17 ± 0.60 at the lowest leaf temperature and 1.32 ± 0.81
365 at the highest leaf temperature (**Fig. 2**). In addition, Fv'/Fm' remained stable as leaf temperatures
366 increased with a variation of less than 1%, with a value of 0.57 ± 0.02 at the lowest leaf temperature
367 and 0.58 ± 0.05 at the highest leaf temperature (supplementary data, **figure S1**).
368 As summarized in **Table 1**, strong positive correlations (indicated with Pearson's product-
369 moment correlation coefficient, *r*) were observed between leaf isoprene emissions and q_L and ETR.
370 Across the leaf temperature response curves, mean isoprene emissions were nearly perfectly
371 linearly correlated with mean values of ETR (r = 0.98) and qL (r = 0.99). In contrast, leaf isoprene
372 emissions were strongly negatively correlated with g_s (r = -0.97) and C_i (r = -0.97). Following
373 regression analysis, linear equations and coefficients of determination (R^2) were determined
374 between isoprene emissions and the photochemical parameters ETR (μmol e^- m^{-2} s^{-1}) and q_L as
375 follows:
376 **Eq.7**. Isoprene emissions = (0.37 ± 0.03) ETR - 49.1 ± 4.19 (R^2 = 0.97)

Eq.8. Isoprene emissions = (126.26 ± 6.57) q_L + 38.875 ± 2.89 (R^2 = 0.98)

3.2 Isoprene inhibitor studies

In order to test whether the isoprenoid pathway is necessary to maintain high photosynthetic rates at elevated temperatures, we applied the isoprenoid biosynthesis inhibitor fosmidomycin to detached branches as a solution delivered to leaves via the transpiration stream. Fosmidomycin application resulted in the complete loss of isoprene emissions at all leaf temperatures (**Fig. 3a**). In contrast, under water fed control branches, leaf isoprene emission continued to be stimulated through the highest leaf temperatures achievable (47.9 ± 2.0°C). It should be noted, that because the inhibitor experiments occurred during the dry season with greatly reduced cloud cover, the maximum leaf temperatures achievable were much higher than in the chlorophyll florescence experiments (**Figs. 1-2**), which occurred during the wet season with a greater degree of cloud cover. Fosmidomycin treated branches showed reduced g_s relative to water fed controls (**Fig. 3d**). This reduction of g_s caused a temperature independent reduction in P_n in the fosmidomycin treated leaves, reducing the values by up to 40% relative to the water fed control (**Fig. 3b**). However, for both water fed control and fosmidomycin treated leaves, both g_s and P_n reached steady state at each temperature throughout the leaf temperature response curve. Moreover, clear temperature dependent trends can be discerned from this dataset. For instance, at the lowest leaf temperature (25.4 ± 1.2°C), mean P_n of fosmidomycin fed branches decreased by 64% relative to water controls (14.3 ± 3.8 μmol m^{-2} s^{-1} under water versus 5.2 ± 1.1 μmol m^{-2} s^{-1} under fosmidomycin), while at the highest leaf temperature studied (47.9 ± 2.0°C) mean P_n of fosmidomycin fed branches decreased by 82.8% relative to water controls (8.7 ± 1.5 μmol m^{-2} s^{-1} versus 1.5 ±1.1 μmol m^{-2} s^{-1} under fosmidomycin). Intercellular CO_2 concentrations (C_i, **Fig. 3c**) were similar between the fosmidomycin fed branches and the water fed controls at low leaf

temperatures, however, they diverged at leaf temperatures above 32.5°C. Above these leaf temperatures, C_i values of fosmidomycin fed branches were higher than water fed controls in spite of the low g_s values, consistent with reduced photosynthetic capacity (**Fig. 3b**). Finally, when P_n was normalized by g_s, the temperature dependent effect of the inhibitor on photosynthesis can be clearly observed (P_n/g_s, **Fig. 4**). At low temperatures, P_n/g_s was indistinguishable between the water fed control branches and the fosmidomycin fed branches (25.4 ± 1.2°C). At high temperatures, P_n/g_s was lower in the fosmidomycin fed branches relative to the water fed controls as leaf temperature increased. The largest reduction in P_n/g_s was observed at the highest leaf temperature (47.9 ± 2.0°C) where P_n/g_s was reduced by 35.8%. Thus, by inhibiting isoprenoid biosynthesis, photosynthetic capacity is reduced at high temperatures in *V. guianensis.*

4. Discussion

Current mechanistic isoprene emission models predict that high temperatures are associated with an enhanced rate of the production of the energetic and reductive equivalents necessary for isoprenoid biosynthesis generated by the photochemical phase of photosynthesis. However, even though tropical forests are the largest global source of isoprene in the atmosphere, whether the link between high ETR and isoprene emission is valid in tropical trees had not been tested. We lacked a quantitative assessment of the relationship between ETR and isoprene emissions in the tropics.

Using coupled gas exchange, chlorophyll fluorescence, and isoprene emission observations during controlled leaf temperature response curves of *V. guianensis*, an early successional species in the central Amazon, we provide evidence that temperature induced stimulation of isoprene emissions is tightly correlated with ETR and q_L, both of which indicate a stimulation in the rate of light-dependent NADPH and ATP production in the chloroplast (Niinemets *et al.*, 2002a,b). We observed this strong temperature stimulation, and a near perfect coupling between isoprene

emissions and ETR and q_L, despite a decline in g_s and P_n at high temperatures. The high temperatures did not alter the maximum photochemical efficiency of PSII as demonstrated by a near constant Fv'/Fm' (supplementary data, **figure S1**) value of 0.57 over the range of the entire leaf temperature measurement regime, nor were other photoprotective mechanisms, such as NPQ, induced under these conditions. Assisted by solar heating of the leaf chamber during the Amazon dry season, leaf temperatures during controlled temperature response curves reached values up to 50°C with isoprene emissions continuing to increase (see **Fig. 3**). Thus, rather than scaling down the photochemical reactions of photosynthesis at high temperatures and increasing NPQ rates, the photochemical reactions of *V. guianensis* leaves continue to increase likely through a tight coupling to increased demand by non-CO_2 consuming metabolic pathways for photochemically generated NADPH and/or ATP at high temperatures. This provides direct evidence that suppression of P_n at high leaf temperatures in the tropics is mainly associated with reductions in g_s rather than direct negative temperature effects on photosynthesis itself (Lloyd & Farquhar, 2008) and is consistent with a previous study that observed a negative correlation between isoprene emissions and NPQ (Pollastri *et al.*, 2014). Recently, isoprene photoprotection of photosynthesis has been described through mechanisms alternative to NPQ, enabling plants to maintain a high photosynthetic rates at rising temperatures by maintaining PSII and thylakoid membrane stability (Pollastri *et al.*, 2019).

Notably, our results with *V. guianensis* stand in contrast to other studies including field-grown cotton plants (a non-isoprene emitter) in North America, which regularly experience temperatures of 40°C or higher during the growing season. It has been reported that components of the photosynthetic apparatus in cotton leaves experience damage at high temperatures (35–42°C) (Wise *et al.*, 2004). In a study carried out with the tropical tree *Inga edulis* in the central

Amazon (an isoprene emitter), it was observed that the rate of ETR declined after reaching 28-36°C (Mendes *et al.*, 2017). Similar results were found in four species in a Malaysian rainforest, where ETR declined after reaching a 35°C (Kitao *et al.*, 2000) and in a rainforest in Rwanda where three species showed a decrease in ETR at leaf temperatures beyond 30°C and other three species showed ETR declines above 35-37°C (Vårhammar *et al.*, 2015). As isoprene emissions were not quantified in these studies, further studies are needed to determine if the continuous stimulation of ETR and isoprene emissions to extreme leaf temperatures is a unique functional trait characteristic of *V. guianensis*, or also a common occurrence in other early and late successional species in the tropics that are regularly exposed to full sun and extreme daytime temperatures.

While the atmospheric roles of isoprene have been extensively investigated (Grosjean *et al.*, 1993), much less is known about its biological roles including potential direct and indirect impacts on the terrestrial carbon cycle during climate warming. Directly, leaf isoprene emissions to the atmosphere represent a small (e.g. 5% at a leaf temperature of 50°C, **Fig. 3**), but potentially important loss of carbon from tropical forests as surface temperatures increase (Harley *et al.*, 1996). In addition to this direct impact on the carbon cycle through a loss of ecosystem carbon, our results are consistent with a secondary effect; isoprene production at high temperatures may minimize the suppression in P_n during high temperature extremes, and improve recovery rates once more favorable temperatures are encountered (Sharkey *et al.*, 2001). This is supported by the observations that blocking the isoprenoid pathway with fosmidomycin in *V. guianensis* repressed P_n at high temperatures through a mechanism that was independent of stomatal closure (**Figs. 3-4**). Whether this is a consequence of the direct thermoprotective and signaling effects of isoprene itself or other isoprenoid intermediates and products, or the loss of a major chloroplastic NADPH and ATP consuming pathway at high temperatures will be a focus of future work. Although

fosmidomycin is considered highly specific and does not directly inhibit photosynthesis (Sharkey *et al.*, 2001), it has been shown to rapidly (with 1 hour) reduce P_n, PSII chlorophyll fluorescence, V_{cmax} (the maximum rate of Ribulose-1,5-bisphosphate carboxylase activity) and J_{max} (the maximum rate of photosynthetic electron transport) (Possell *et al.*, 2010). Thus, care should be taken in attributing these effects solely to a lack of isoprene as fosmidomycin negatively impacts the synthesis of numerous other isoprenoids involved in photosynthesis resulting in photoinhibition and photo-damage (Possell *et al.*, 2010). However, that the direct inhibition of photosynthetic capacity with fosmidomycin in this experiment was only observed at temperatures well in excess of the optimum P_n temperature is consistent with the role of isoprene in maintaining high photosynthetic capacity under thermal stress conditions in tropical species. A recent literature survey of tropical plants reported that maximum temperatures for P_n ~1.8°C higher for isoprene-emitting species than for non-emitters, and thermal response curves were 24% wider (Taylor *et al.*, 2019). Consistent with a significant impact on the ability of tropical forests to maintain a strong carbon sink throughout the 21st century, this study suggested that isoprene emission may be an adaptation to warmer thermal niches, and that emitting species may fare better under global warming than co-occurring non-emitting species. However, the direct and indirect impacts of isoprene emission on terrestrial carbon cycling in the tropics during high temperature extremes remains to be quantified.

As isoprene emissions itself may represent a small fraction of ETR (Lantz *et al.*, 2019), we estimated this fraction by using the slope of the linear relationship in **Eq. 7** (0.37 nmol isoprene/μmol e^-). Thus, we estimate that as temperatures vary, the percentage of electrons leading to isoprene biosynthesis is 0.037%. Thus, it is important to note that even at high temperatures, only a small fraction of the reducing equivalents generated by ETR will be directly consumed for

492 isoprene biosynthesis and the strong coupling of ETR/q_L and isoprene biosynthesis must be
493 supported by the induction of other pathways that consume the bulk of photosynthetically-derived
494 NADPH and ATP including the biosynthesis of non-volatile isoprenoids as well as other linked
495 biochemical processes and pathways such as photorespiration (Voss *et al.*, 2013), the re-
496 assimilation of respiratory and photorespiratory CO_2 (Garcia *et al*., 2019), the malate valve
497 (Rasulov *et al.*, 2018), mitochondrial respiration (Loreto *et al.*, 2007), and the alternate oxidase
498 pathway (Atkin & Tjoelker, 2003) (**Fig. 5**). For example, as leaf temperatures increase,
499 photorespiration rates rise faster than photosynthetic rates and an increasing proportion of the
500 NADPH and ATP are diverted into photorespiration (Long, 1991). Moreover, as temperatures
501 increase a large fraction of photorespiratory CO_2 can be re-assimilated by photosynthesis (Voss *et*
502 *al.*, 2013) and photorespiratory intermediates are increasingly incorporated into isoprene emissions
503 (Jardine *et al.*, 2014). Thus, despite isoprene emissions representing a small fraction of ETR (e.g.
504 0.037%), our observations are consistent with a mechanism where isoprenoid biosynthesis
505 operates in parallel with numerous coupled pathways which accelerate under high temperature to
506 create a positive feedback with ETR to maintain high photosynthetic capacity.

507 Previous research suggested that large variations in isoprene emissions as a function of
508 light, CO_2, temperature and oxygen were driven by the energy status of chloroplasts (Rasulov *et*
509 *al.*, 2009; Morfopoulos *et al.*, 2013); a result predicted by models of plant isoprene emissions based
510 on available NADPH and ATP (Morfopoulos *et al.*, 2013, 2014). These mechanisms have been
511 incorporated into Earth system models (Pacifico *et al.*, 2011; Harrison *et al.*, 2013) which predict
512 regional to global emission patterns of isoprene linked to photosynthesis. Therefore, the
513 quantitative relationship presented here between ETR and isoprene emissions from an abundant
514 Neotropical early successional species can be used in future modeling studies to improve the

accuracy of simulations predicting large increases in tropical isoprene emissions associated with increased forest dynamics and climate warming.

The optimal temperature range for P_n has been cited as 30-31°C as typical for climax tree species in terra-firme tropical forests (Lloyd & Farquhar, 2008; Jardine *et al.*, 2017a; Slot & Winter, 2017). For example, in Panama reported optimum temperatures for P_n ranged from 28.4°C to 31.9°C without a significant difference detected between trees and lianas and dry and wet sites. Thus, *V. guianensis* appears to show a higher optimum temperature for P_n than previously reported for tropical species (32.6 ± 0.4°C). Moreover, isoprene emissions continued to increase through the highest temperatures obtainable by the leaf gas exchange system (wet season greater than or equal to 38.3 ± 0.4°C: **Figs. 1-2**, dry season 48.1 ± 2.0°C: **Fig. 3**). Thus, *V. guianensis* shows a dramatically higher optimum temperature for isoprene emissions than reported for other species (up to 10°C higher). To our knowledge, this represents the highest reported leaf temperature by which isoprene emissions continue to be stimulated by increasing temperature. These findings suggest that the photosynthetic apparatus in *V. guianensis,* and its coupling to isoprene production, is well adapted to the extreme high temperatures regularly experienced in secondary forests, in which the leaf temperature in the middle of the day and early afternoon regularly exceeds the ideal temperature range for P_n (Doughty & Goulden, 2008), especially during the dry season and during droughts. For example, during the dry season of 2015-16 in a central Amazon rainforest, the upper canopy reached leaf temperatures > 45°C with strong afternoon suppression of P_n associated with partial stomatal closure (Jardine et al., 2017a). A previous study with poplar leaves observed that the temperature optimum for P_n (30^oC) < ETR (35^oC) < isoprene emissions (45^oC) < enzyme activity of isoprene synthase (50^oC) (Monson *et al.*, 1992). Thus, in order to determine the full extent of coupling of ETR and isoprene emission, future studies using engineered gas exchange

538 systems capable of extreme leaf temperatures (e.g. 25-60^{o}C) should be used to determine at what
539 temperature ETR and isoprene emissions from *V. guianensis* finally begin to decline and if ETR
540 and isoprene emissions share the same optimum leaf temperature.

541 As remote sensing of gross primary productivity using solar induced fluorescence (Yang
542 *et al.*, 2015) and isoprene emissions (both direct isoprene observations and indirect via atmospheric
543 formaldehyde columns measurements) (Zheng *et al.*, 2015; Fu *et al.*, 2019) are being evaluated
544 from ecosystem to global scales, our mechanistic results may be utilized to better understand
545 integrative studies on terrestrial carbon cycling in the tropics. For example, when atmospheric
546 formaldehyde was used as a proxy for tropical isoprene emissions, it was found that isoprene
547 emissions tracked the seasonal cycle of canopy temperature, but was anticorrelated with gross
548 primary productivity (Foster *et al.*, 2014). In light of our leaf level observations, this could be
549 explained by an increase in isoprene emissions and photochemical reactions of photosynthesis at
550 high temperatures, but a suppression of P_n associated with partial stomatal closure.

551

552 **5. Acknowledgements**

553 This material is based upon work supported as part of the Next Generation Ecosystem
554 Experiments-Tropics (NGEE-Tropics) funded by the U.S. Department of Energy, Office of
555 Science, Office of Biological and Environmental Research`s Terrestrial Ecosystem Science
556 Program through contract No. DE-AC02-05CH11231 to Lawrence Berkeley National Laboratory,
557 DE-AC05-00OR22725 to Oak Ridge National Laboratory, and DE-SC0012704 to Brookhaven
558 National Laboratory. Additional funding for this research was provided by the Brazilian Conselho
559 Nacional de Desenvolvimento Científico e Tecnológico (CNPq). Logistical and scientific support
560 is acknowledged by the Forest Management laboratory (LMF), Climate and Environment

561 (CLIAMB), and Large Scale Biosphere-Atmosphere (LBA) programs at the National Institute for
562 Amazon Research (INPA).

563

564 **6. References**

565 Affek HP, Yakir D (2003) Natural abundance carbon isotope composition of isoprene reflects
566 incomplete coupling between isoprene synthesis and photosynthetic carbon flow. *Plant*
567 *Physiology*, **131**, 1727–1736. DOI:10.1104/pp.102.012294
568 Alves EG, Harley P, Gonçalves JF de C, Moura CE da S, Jardine K (2014) Effects of light and
569 temperature on isoprene emission at different leaf developmental stages of eschweilera
570 coriacea in central Amazon. *Acta amazonica*, **44**, 9–18. DOI:10.1590/S0044-
571 59672014000100002
572 Atkin OK, Tjoelker MG (2003) Thermal acclimation and the dynamic response of plant
573 respiration to temperature. *Trends in Plant Science*, **8**, 343–351. DOI: 10.1016/S1360-
574 1385(03)00136-5
575 Baker NR, Rosenqvist E (2004) Applications of chlorophyll fluorescence can improve crop
576 production strategies: an examination of future possibilities. *Journal of Experimental*
577 *Botany*, **55**, 1607–1621. DOI: 10.1093/jxb/erh196
578 Beer C, Reichstein M, Tomelleri E et al. (2010) Terrestrial gross carbon dioxide uptake: global
579 distribution and covariation with climate. *Science*, **329**, 834–838. DOI:
580 10.1126/science.1184984
581 Brienen RJW, Phillips OL, Feldpausch TR et al. (2015) Long-term decline of the Amazon carbon
582 sink. *Nature*, **519**, 344–348. DOI: 10.1038/nature14283
583 Chambers JQ, Silver WL (2004) Some aspects of ecophysiological and biogeochemical
584 responses of tropical forests to atmospheric change. *Philosophical Transactions of the*
585 *Royal Society of London. Series B, Biological Sciences*, **359**, 463–476. DOI:
586 10.1098/rstb.2003.1424
587 Chambers JQ, Robertson AL, Carneiro VMC, Lima AJN, Smith M-L, Plourde LC, Higuchi N
588 (2009) Hyperspectral remote detection of niche partitioning among canopy trees driven by
589 blowdown gap disturbances in the Central Amazon. *Oecologia*, **160**, 107–117. DOI:
590 10.1007/s00442-008-1274-9
591 Dani KGS, Jamie IM, Prentice IC, Atwell BJ (2015) Species-specific photorespiratory rate,
592 drought tolerance and isoprene emission rate in plants. *Plant Signaling & Behavior*, **10**,
593 e990830. DOI: 10.4161/15592324.2014.990830
594 Delwiche CF, Sharkey TD (1993) Rapid appearance of 13C in biogenic isoprene when 13CO2
595 is fed to intact leaves. *Plant, Cell & Environment*, **16**, 587–591. DOI: 10.1111/j.1365-
596 3040.1993.tb00907.x
597 Doughty CE, Goulden ML (2008) Are tropical forests near a high temperature threshold?
598 *Journal of Geophysical Research: Biogeosciences*, **113**. DOI:10.1029/2007JG000632
599 Duncan BN, Yoshida Y, Damon MR, Douglass AR, Witte JC (2009) Temperature dependence
600 of factors controlling isoprene emissions. *Geophysical Research Letters*, **36**. DOI:
601 10.1029/2008GL037090
602 Earl HJ, Tollenaar M (1998) Relationship between thylakoid electron transport and
603 photosynthetic CO2 uptake in leaves of three maize (Zea mays L.) hybrids. *Photosynthesis*
604 *Research*. DOI: 10.1023/A:1006198821912
605 Foster PN, Prentice IC, Morfopoulos C (2014) Isoprene emissions track the seasonal cycle of
606 canopy temperature, not primary production: evidence from remote sensing.
607 *Biogeosciences*, **11**, 3437–3451. DOI:10.5194/bg-11-3437-2014

608 Funk JL, Mak JE, Lerdau MT (2004) Stress-induced changes in carbon sources for isoprene
609 production in Populus deltoides. *Plant, Cell & Environment*, **27**, 747–755. DOI:
610 10.1111/j.1365-3040.2004.01177.x
611 Fu D, Millet DB, Wells KC, Payne VH, Yu S, Guenther A, Eldering A (2019) Direct retrieval of
612 isoprene from satellite-based infrared measurements. *Nature Communications*, **10**, 3811.
613 DOI: 10.1038/s41467-019-11835
614 Garcia S, Jardine K, Souza V, Souza R, Duvoisin Junior S, Gonçalves J (2019) Reassimilation
615 of Leaf Internal CO2 Contributes to Isoprene Emission in the Neotropical Species *Inga*
616 *edulis* Mart. *Forests*, **10**, 472. DOI: 10.3390/f10060472
617 Goulden ML, Miller SD, da Rocha HR, Menton MC, de Freitas HC, e Silva Figueira AM, de
618 Sousa CAD (2004) Diel and seasonal patterns of tropical forest CO_2 exchange. Ecological
619 Applications, **14**, 42–54. DOI: 10.1890/02-6008
620 Grosjean D, Williams EL, Grosjean E (1993) Atmospheric chemistry of isoprene and of its
621 carbonyl products. *Environmental science & technology*, **27**, 830–840. DOI:
622 10.1021/es00042a004
623 Guenther A, Karl T, Harley P, Wiedinmyer C, Palmer PI, Geron C (2006) Estimates of global
624 terrestrial isoprene emissions using MEGAN (Model of Emissions of Gases and Aerosols
625 from Nature). *Atmospheric Chemistry and Physics*, **6**, 3181–3210. DOI: 10.5194/acp-6-
626 3181-2006
627 Guidolotti G, Pallozzi E, Gavrichkova O, Scartazza A, Mattioni M, Loreto F, Calfapietra C (2019)
628 Emission of constitutive isoprene, induced monoterpenes, and other volatiles under hight
629 temperatures in *Eucalyptus camaldulensis*: A ^{13}C labelling study. *Plant, Cell & Environment*,
630 **42**, 1929-1938. DOI: 10.1111/pce.13521
631 Harley P, Guenther A, Zimmerman P (1996) Effects of light, temperature and canopy position
632 on net photosynthesis and isoprene emission from sweetgum (Liquidambar styraciflua)
633 leaves. *Tree Physiology*, **16**, 25–32. DOI: 10.1093/treephys/16.1-2.25
634 Harley PC, Monson RK, Lerdau MT (1999) Ecological and evolutionary aspects of isoprene
635 emission from plants. *Oecologia*, **118**, 109–123. DOI: 10.1007/s004420050709
636 Harrison SP, Morfopoulos C, Dani KGS et al. (2013) Volatile isoprenoid emissions from plastid
637 to planet. *The New Phytologist*, **197**, 49–57. DOI: 10.1111/nph.12021
638 Higuchi N, dos Santos J, Vieira G et al. (1998) Análise estrutural da floresta primária da bacia
639 do rio Cuieiras, ZF-2, Manaus-AM, Brasil. *Acta Amazonica*, **28**, 153–166.
640 Himalayan O, Tech B (2005) Physiological basis of seasonal trend in leaf photosynthesis of five
641 evergreen broad-leaved species in a temperate deciduous forest. *Tree Physiology*, **4**, 249–
642 256. DOI: 10.1093/treephys/26.2.249
643 Ishida A, Toma T (1999) Limitation of leaf carbon gain by stomatal and photochemical
644 processes in the top canopy of. *Tree Physiology*. DOI: 10.1093/treephys/19.7.467
645 Jardine KJ, Sommer ED, Saleska SR, Huxman TE, Harley PC, Abrell L (2010) Gas phase
646 measurements of pyruvic acid and its volatile metabolites. *Environmental science &*
647 *technology*, **44**, 2454–2460. DOI: 10.1021/es903544p
648 Jardine K, Yañez Serrano A, Arneth A et al. (2011) Within-canopy sesquiterpene ozonolysis in
649 Amazonia. *Journal of Geophysical Research*, **116**. DOI: 10.1029/2011JD016243
650 Jardine KJ, Monson RK, Abrell L et al. (2012) Within-plant isoprene oxidation confirmed by
651 direct emissions of oxidation products methyl vinyl ketone and methacrolein. *Glob Change*
652 *Biol*, **18**, 973–984. DOI: 10.1111/j.1365-2486.2011.02610.x
653 Jardine K, Chambers J, Alves EG et al. (2014) Dynamic balancing of isoprene carbon sources
654 reflects photosynthetic and photorespiratory responses to temperature stress. *Plant*
655 *Physiology*, **166**, 2051–2064. DOI: https://doi.org/10.1104/pp.114.247494
656 Jardine AB, Jardine KJ, Fuentes JD et al. (2015a) Highly reactive light-dependent
657 monoterpenes in the Amazon. *Geophysical Research Letters*, **42**, 1576–1583. DOI:
658 10.1002/2014GL062573

659 Jardine KJ, Chambers JQ, Holm J et al. (2015b) Green Leaf Volatile Emissions during High
660 Temperature and Drought Stress in a Central Amazon Rainforest. *Plants*, **4**, 678–690. DOI:
661 10.3390/plants4030678
662 Jardine KJ, Jardine AB, Souza VF et al. (2016) Methanol and isoprene emissions from the fast
663 growing tropical pioneer species *Vismia guianensis* (Aubl.) Pers. (Hypericaceae) in the
664 central Amazon forest. *Atmospheric Chemistry and Physics*, **16**, 6441–6452. DOI:
665 10.5194/acp-16-6441-2016
666 Jardine KJ, Jardine AB, Holm JA et al. (2017a) Monoterpene "thermometer" of tropical forest-
667 atmosphere response to climate warming. *Plant, Cell & Environment*, **40**, 441–452. DOI:
668 10.1104/pp.102.012294
669 Jardine KJ, Fernandes de Souza V, Oikawa P et al. (2017b) Integration of C_1 and C_2
670 metabolism in trees. *International Journal of Molecular Sciences*, **18**. DOI:
671 10.3390/ijms18102045
672 [dataset] Jardine K; Rodrigues T (2019): Isoprene, Chlorophyll fluorescence, and leaf
673 temperature data from Manaus, Brazil, 2017 - 2018. 1.0. NGEE Tropics Data Collection.
674 (dataset). http://dx.doi.org/10.15486/ngt/1570407
675 Karl T, Guenther A, Turnipseed A, Tyndall G, Artaxo P, Martin S (2009) Rapid formation of
676 isoprene photo-oxidation products observed in Amazonia. *Atmospheric Chemistry and*
677 *Physics*, **9**, 7753–7767. DOI: 10.5194/acp-9-7753-2009
678 Karl T, Harley P, Emmons L et al. (2010) Efficient atmospheric cleansing of oxidized organic
679 trace gases by vegetation. *Science*, **330**, 816–819. DOI: 10.1126/science.1192534
680 Kitao M, Lei TT, Koike T, Tobita H, Maruyama Y, Matsumoto Y, Ang L-H (2000) Temperature
681 response and photoinhibition investigated by chlorophyll fluorescence measurements for
682 four distinct species of dipterocarp trees. *Physiologia Plantarum*, **109**, 284–290. DOI:
683 10.1034/j.1399-3054.2000.100309.x
684 Koch GW, Amthor JS., Goulden ML (1994) Diurnal patterns of leaf photosynthesis, conductance
685 and water potential at the top fo a lowland rain forest canopy in cameroon: measurements
686 from the Radeau des Cimes. *Tree Physiology*, **14**, 347–360. DOI:
687 10.1093/treephys/14.4.347
688 Koren G, van Schaik E, Araújo AC et al. (2018) Widespread reduction in sun-induced
689 fluorescence from the Amazon during the 2015/2016 El Niño. *Philosophical Transactions of*
690 *the Royal Society of London. Series B, Biological Sciences*, **373**. DOI:
691 10.1098/rstb.2017.0408
692 Kramer DM, Johnson G (2004) Kiirats 0, et al. New Fluorescence Parame-ters for the
693 Determination of QA Redox State and Excitation EnergyFluxes. *Photosynthesis Research*,
694 **79**, 209–218. DOI: 10.1023/B:PRES.0000015391.99477.0d
695 Krause GH, Weis E (1984) Chlorophyll fluorescence as a tool in plant physiology: II.
696 Interpretation of fluorescence signals. *Photosynthesis Research*, **5**, 139–157. DOI:
697 10.1007/BF00028527
698 Kreuzwieser J, Graus M, Wisthaler A, Hansel A, Rennenberg H, Schnitzler J-P (2002) Xylem-
699 transported glucose as an additional carbon source for leaf isoprene formation in Quercus
700 robur. *The New Phytologist*, **156**, 171–178. DOI: 10.1046/j.1469-8137.2002.00516.x
701 Lantz AT, Allman J, Weraduwage SM, Sharkey TD (2019) Isoprene: New insights into the
702 control of emission and mediation of stress tolerance by gene expression. *Plant, Cell &*
703 *Environment*, **42**, 2808–2826. DOI: 10.1111/pce.13629
704 Lichtenthaler HK (1999) The 1-Deoxy-D-Xylulose-5-Phosphate Pathway of Isoprenoid
705 Biosynthesis in Plants. *Annual review of plant physiology and plant molecular biology*, **50**,
706 47–65. DOI: 10.1146/annurev.arplant.50.1.47
707 Liu J, Bowman KW, Schimel DS et al. (2017) Contrasting carbon cycle responses of the tropical
708 continents to the 2015-2016 El Niño. *Science*, **358**. DOI: 10.1126/science.aam5690

709 Li Z, Wakao S, Fischer BB, Niyogi KK (2009) Sensing and responding to excess light. *Annual*
710 *review of plant biology*, **60**, 239–260. DOI: 10.1146/annurev.arplant.58.032806.103844
711 Li Z, Ratliff EA, Sharkey TD (2011) Effect of temperature on postillumination isoprene emission
712 in oak and poplar. *Plant Physiology*, **155**, 1037–1046. DOI: 10.1104/pp.110.167551
713 Lloyd J, Farquhar GD (2008) Effects of rising temperatures and [CO2] on the physiology of
714 tropical forest trees. *Philosophical Transactions of the Royal Society of London. Series B,*
715 *Biological Sciences*, **363**, 1811–1817. DOI: 10.1098/rstb.2007.0032
716 Long SP (1991) Modification of the response of photosynthetic productivity to rising temperature
717 by atmospheric CO_2 concentrations: Has its importance been underestimated? *Plant, Cell &*
718 *Environment*, **14**, 729–739. DOI: 10.1111/j.1365-3040.1991.tb01439.x
719 Loreto F, Sharkey TD (1990) A gas-exchange study of photosynthesis and isoprene emission
720 inQuercus rubra L. *Planta*, **182**, 523–531. DOI: 10.1007/BF02341027
721 Loreto F, Centritto M, Barta C, Calfapietra C, Fares S, Monson RK (2007) The relationship
722 between isoprene emission rate and dark respiration rate in white poplar (*Populus alba* L.)
723 leaves. *Plant, Cell & Environment*, **30**, 662–669. DOI: 10.1111/j.1365-3040.2007.01648.x
724 Mendes KR, Marenco RA, Nascimento HCS (2017) Maximum carboxylation velocity of
725 RUBISCO and maximum rate of electron transport in saplings in response to variations in
726 environmental factors in central Amazonia. *Ciência Florestal*, **27**, 947–959.
727 Mesquita RCG, Delamônica P, Laurance WF (1999) Effect of surrounding vegetation on edge-
728 related tree mortality in Amazonian forest fragments. *Biological Conservation*, **91**, 129–134.
729 DOI: 10.1016/S0006-3207(99)00086-5
730 Mesquita R de CG, Massoca PE dos S, Jakovac CC, Bentos TV, Williamson GB (2015)
731 Amazon Rain Forest Succession: Stochasticity or Land-Use Legacy? *Bioscience*, **65**, 849–
732 861. DOI: 10.1093/biosci/biv108
733 Mittler R (2017) ROS Are Good. *Trends in Plant Science*, **22**, 11–19. DOI:
734 10.1016/j.tplants.2016.08.002
735 Monson RK, Jaeger CH, Adams WW, Driggers EM, Silver GM, Fall R (1992) Relationships
736 among Isoprene Emission Rate, Photosynthesis, and Isoprene Synthase Activity as
737 Influenced by Temperature. *Plant Physiology*, **98**, 1175–1180. DOI: 10.1104/pp.98.3.1175
738 Morfopoulos C, Prentice IC, Keenan TF, Friedlingstein P, Medlyn BE, Peñuelas J, Possell M
739 (2013) A unifying conceptual model for the environmental responses of isoprene emissions
740 from plants. *Annals of Botany*, **112**, 1223–1238. DOI: 10.1093/aob/mct206
741 Morfopoulos C, Sperlich D, Peñuelas J et al. (2014) A model of plant isoprene emission based
742 on available reducing power captures responses to atmospheric CO_2. *New Phytologist*,
743 **203**, 125–139. DOI: 10.1111/nph.12770
744 Müller P, Li XP, Niyogi KK (2001) Non-photochemical quenching. A response to excess light
745 energy. *Plant Physiology*, **125**, 1558–1566. DOI: 10.1104/pp.125.4.1558
746 Murchie EH, Lawson T (2013) Chlorophyll fluorescence analysis: a guide to good practice and
747 understanding some new applications. *Journal of Experimental Botany*, **64**, 3983–3998.
748 DOI: 10.1093/jxb/ert208
749 Niinemets U, Hauff K, Bertin N, Tenhunen JD, Steinbrecher R, Seufert G (2002a) Monoterpene
750 emissions in relation to foliar photosynthetic and structural variables in Mediterranean
751 evergreen Quercus species. *The New Phytologist*, **153**, 243–256. DOI: 10.1046/j.0028-
752 646X.2001.00323.x
753 Niinemets U, Seufert G, Steinbrecher R, Tenhunen JD (2002b) A model coupling foliar
754 monoterpene emissions to leaf photosynthetic characteristics in Mediterranean evergreen
755 Quercus species. *The New Phytologist*, **153**, 257–275. DOI: 10.1046/j.0028-
756 646X.2001.00324.x
757 Pacifico F, Harrison SP, Jones CD, Sitch S (2009) Isoprene emissions and climate.
758 *Atmospheric environment*, **43**, 6121–6135. DOI: 10.1016/j.atmosenv.2009.09.002

759 Pacifico F, Harrison SP, Fu TM et al. (2011) Evaluation of a photosynthesis-based biogenic
760 isoprene emission scheme in JULES and simulation of isoprene emissions under present-
761 day climate conditions. DOI:10.5194/acp-11-4371-2011
762 Piedade MTF, Long SP, Junk WJ (1994) Leaf and canopy photosynthetic CO_2 uptake of a stand
763 of Echinochloa polystachya on the Central Amazon floodplain: Are the high potential rates
764 associated with the C4 syndrome realized under the near-optimal conditions provided by
765 this exceptional natural habitat? *Oecologia*, **97**, 193–201. DOI: 10.1007/BF00323149
766 Pollastri S, Tsonev T, Loreto F (2014) Isoprene improves photochemical efficiency and
767 enhances heat dissipation in plants at physiological temperatures. *Journal of Experimental*
768 *Botany*, **65**, 1565–1570. DOI: 10.1093/jxb/eru033
769 Pollastri S, Jorba I, Hawkins TJ et al. (2019) Leaves of isoprene-emitting tobacco plants
770 maintain PSII stability at high temperatures. *The New Phytologist*, **223**, 1307–1318. DOI:
771 10.1111/nph.15847
772 Possell M, Ryan A, Vickers CE, Mullineaux PM, Hewitt CN (2010) Effects of fosmidomycin on
773 plant photosynthesis as measured by gas exchange and chlorophyll fluorescence.
774 *Photosynthesis Research*, **104**, 49–59. DOI: 10.1007/s11120-009-9504-5
775 Potter C, Klooster S, Hiatt C, Genovese V, Castilla-Rubio JC (2011) Changes in the carbon
776 cycle of Amazon ecosystems during the 2010 drought. *Environmental Research Letters*, **6**,
777 034024. DOI:10.1088/1748-9326/6/3/034024
778 Rapparini F, Baraldi R, Miglietta F, Loreto F (2004) Isoprenoid emission in trees of Quercus
779 pubescens and Quercus ilex with lifetime exposure to naturally high CO_2 environment+.
780 *Plant, Cell & Environment*, **27**, 381–391. DOI: 10.1111/j.1365-3040.2003.01151.x
781 Rasulov B, Hüve K, Välbe M, Laisk A, Niinemets U (2009) Evidence that light, carbon dioxide,
782 and oxygen dependencies of leaf isoprene emission are driven by energy status in hybrid
783 aspen. *Plant Physiology*, **151**, 448–460. DOI: 10.1104/pp.109.141978
784 Rasulov B, Talts E, Bichele I, Niinemets Ü (2018) Evidence that isoprene emission is not limited
785 by cytosolic metabolites. exogenous malate does not invert the reverse sensitivity of
786 isoprene emission to high [CO_2]. *Plant Physiology*, **176**, 1573–1586. DOI:
787 10.1104/pp.17.01463
788 Sage RF, Kubien DS (2007) The temperature response of C(3) and C(4) photosynthesis. *Plant,*
789 *Cell & Environment*, **30**, 1086–1106. DOI: 10.1111/j.1365-3040.2007.01682.x
790 Sanadze GA (1991) Isoprene Effect—Light-Dependent Emission of Isoprene by Green Parts of
791 Plants. In: *Trace gas emissions by plants*, pp. 135–152. Elsevier.
792 Sasaki K, Saito T, Lämsä M et al. (2007) Plants utilize isoprene emission as a thermotolerance
793 mechanism. *Plant & Cell Physiology*, **48**, 1254–1262. DOI: 10.1093/pcp/pcm104
794 Sharkey TD (2005) Effects of moderate heat stress on photosynthesis: importance of thylakoid
795 reactions, rubisco deactivation, reactive oxygen species, and thermotolerance provided by
796 isoprene. *Plant, Cell & Environment*, **28**, 269–277. DOI: 10.1111/j.1365-3040.2005.01324.x
797 Sharkey TD, Yeh S (2001) Isoprene emission from plants. *Annual Review of Plant Physiology*
798 *and Plant Molecular Biology*, **52**, 407–436. DOI: 10.1146/annurev.arplant.52.1.407
799 Sharkey TD, Chen X, Yeh S (2001) Isoprene increases thermotolerance of fosmidomycin-fed
800 leaves. *Plant Physiology*, **125**, 2001–2006. DOI: 10.1104/pp.125.4.2001
801 Silver GM, Fall R (1995) Characterization of aspen isoprene synthase, an enzyme responsible
802 for leaf isoprene emission to the atmosphere. *The Journal of Biological Chemistry*, **270**,
803 13010–13016. DOI: 10.1074/jbc.270.22.13010
804 Singsaas EL, Lerdau M, Winter K, Sharkey TD (1997) Isoprene Increases Thermotolerance of
805 Isoprene-Emitting Species. *Plant Physiology*, **115**, 1413–1420. DOI:
806 10.1104/pp.115.4.1413
807 Slot M, Winter K (2017) In situ temperature response of photosynthesis of 42 tree and liana
808 species in the canopy of two Panamanian lowland tropical forests with contrasting rainfall
809 regimes. *The New Phytologist*, **214**, 1103–1117. DOI: 10.1111/nph.14469

de Souza VF, Niinemets Ü, Rasulov B, Vickers CE, Duvoisin Júnior S, Araújo WL, Gonçalves JF de C (2018) Alternative carbon sources for isoprene emission. *Trends in Plant Science*, **23**, 1081–1101. DOI: 10.1016/j.tplants.2018.09.012

Stutz SS, Hanson DT (2019) Contribution and consequences of xylem-transported CO2 assimilation for C3 plants. *The New Phytologist*, **223**, 1230–1240. DOI: 10.1111/nph.15907

Taylor TC, Smith MN, Slot M, Feeley KJ (2019) The capacity to emit isoprene differentiates the photosynthetic temperature responses of tropical plant species. *Plant, Cell & Environment*, **42**, 2448–2457. DOI: 10.1111/pce.13564

Uhl C, Buschbacher R, Serrao EAS (1988) Abandoned pastures in eastern Amazonia. I. patterns of plant succession. *The Journal of Ecology*, **76**, 663. DOI: 10.2307/2260566

Vårhammar A, Wallin G, McLean CM et al. (2015) Photosynthetic temperature responses of tree species in Rwanda: evidence of pronounced negative effects of high temperature in montane rainforest climax species. *The New Phytologist*, **206**, 1000–1012. DOI: 10.1111/nph.13291

Velikova V, Fares S, Loreto F (2008) Isoprene and nitric oxide reduce damages in leaves exposed to oxidative stress. *Plant, Cell & Environment*, **31**, 1882–1894. DOI: 10.1111/j.1365-3040.2008.01893.x

Vickers CE, Gershenzon J, Lerdau MT, Loreto F (2009a) A unified mechanism of action for volatile isoprenoids in plant abiotic stress. *Nature Chemical Biology*, **5**, 283–291. DOI: 10.1038/nchembio.158

Vickers CE, Possell M, Cojocariu CI et al. (2009b) Isoprene synthesis protects transgenic tobacco plants from oxidative stress. *Plant, Cell & Environment*, **32**, 520–531. DOI: 10.1111/j.1365-3040.2009.01946.x

Voss I, Sunil B, Scheibe R, Raghavendra AS (2013) Emerging concept for the role of photorespiration as an important part of abiotic stress response. *Plant Biology*, **15**, 713–722. DOI: 10.1111/j.1438-8677.2012.00710.x

Wise RR, Olson AJ, Schrader SM, Sharkey TD (2004) Electron transport is the functional limitation of photosynthesis in field-grown Pima cotton plants at high temperature. *Plant, Cell & Environment*, **27**, 717–724. DOI: 10.1111/j.1365-3040.2004.01171.x

Yang X, Tang J, Mustard JF et al. (2015) Solar-induced chlorophyll fluorescence that correlates with canopy photosynthesis on diurnal and seasonal scales in a temperate deciduous forest. *Geophysical Research Letters*, **42**, 2977–2987. DOI: 10.1002/2015GL063201

Zalamea M, González G (2008) Leaf fall phenology in a subtropical wet forest in Puerto Rico: from species to community patterns. *Biotropica*, **40**, 295–304. DOI: 10.1111/j.1744-7429.2007.00389.x

Zheng Y, Unger N, Barkley MP, Yue X (2015) Relationships between photosynthesis and formaldehyde as a probe of isoprene emission. *Atmospheric Chemistry and Physics*, **15**, 8559–8576. DOI:10.5194/acp-15-8559-2015

Zuo Z, Weraduwage SM, Lantz AT et al. (2019) Isoprene acts as a signaling molecule in gene networks important for stress responses and plant growth. *Plant Physiology*, **180**, 124–152. DOI: 10.1104/pp.18.01391

7. Supplementary Material

Supplementary Figure S1 showing mean *V. guianensis* leaf temperature responses of fluorescence parameters including maximum quantum efficiency of PSII photochemistry in the light (Fv`/Fm`) and in the dark (Fv/Fm) is available for download as 'FigureS1_SuppInfo.pdf'.

8. Data Availability Statement

The data that support the findings of this study are openly available in NGEE Tropics Data Collection at http://dx.doi.org/10.15486/ngt/1570407, reference number BR-Ma2. The supplementary data (Size: 11,657 KB) includes raw data obtained from the Licor 6400XT gas exchange system and the TD-GC-MS system for isoprene emission analysis and organized as follows:

Fluorescence experiment folder:

- Gas exchange data (Licor 6400XT files) including fluorescence with leaf number and date
- Isoprene data (TD-GC-MS output files) with leaf number and date

Inhibitor experiment folder:

- Gas exchange data (Licor 6400XT files) and isoprene data (TD-GC-MS output files) with isoprenoid fed inhibitor: Folders separated by date
- Gas exchange data (Licor 6400XT files) and isoprene data (TD-GC-MS files) with water fed control branches: Folders separated by date

874 **9. Figures and Tables**

875

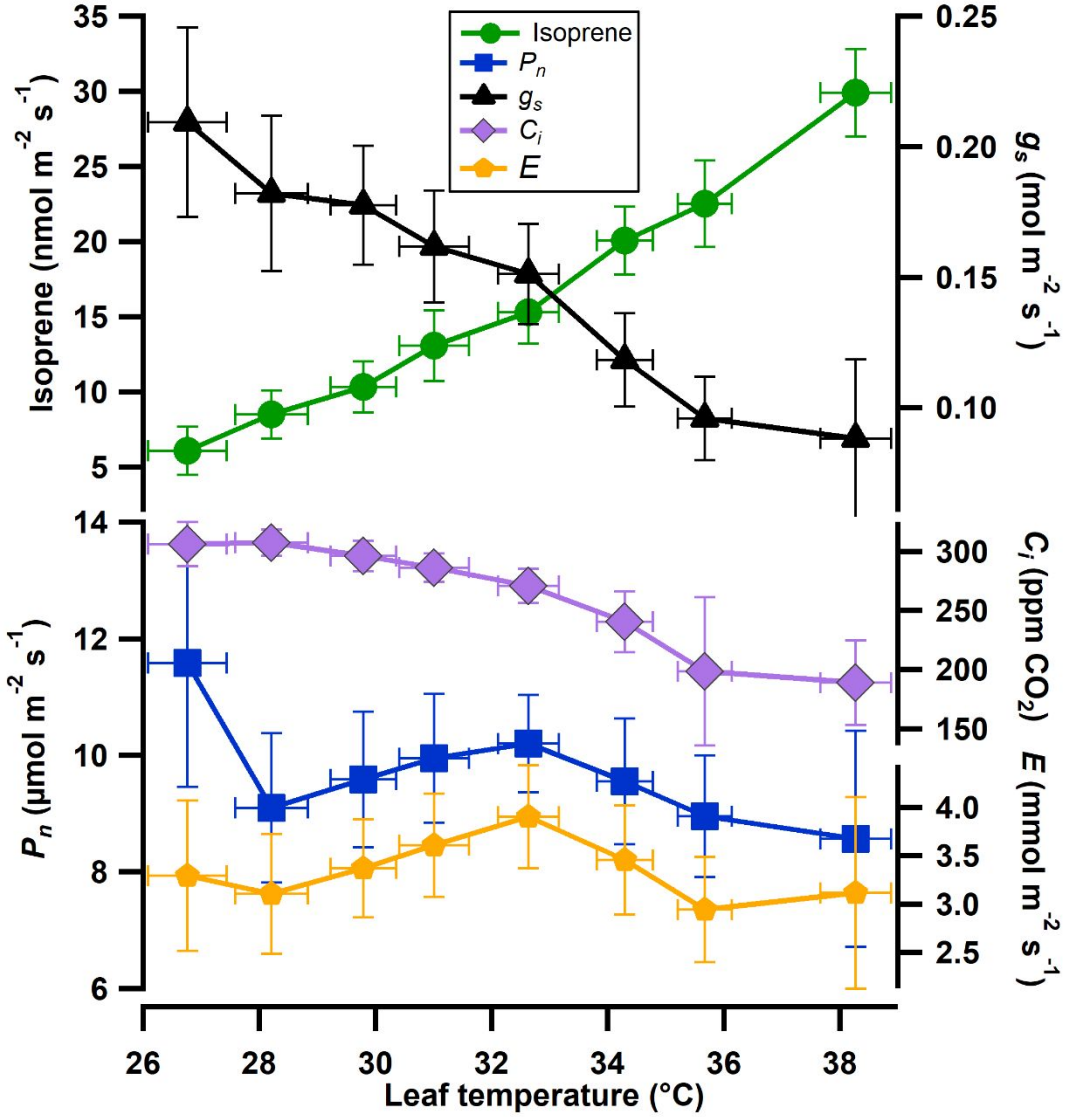

876

877 **Figure 1:** Mean response of net photosynthesis (P_n), stomatal conductance (g_s), internal carbon
878 (C_i), transpiration (E), and isoprene emissions to an increase in leaf temperature in *V. guianensis*.
879 Data shown are the mean of 23 temperature response curves collected with error bars representing
880 ± 2 standard deviation.

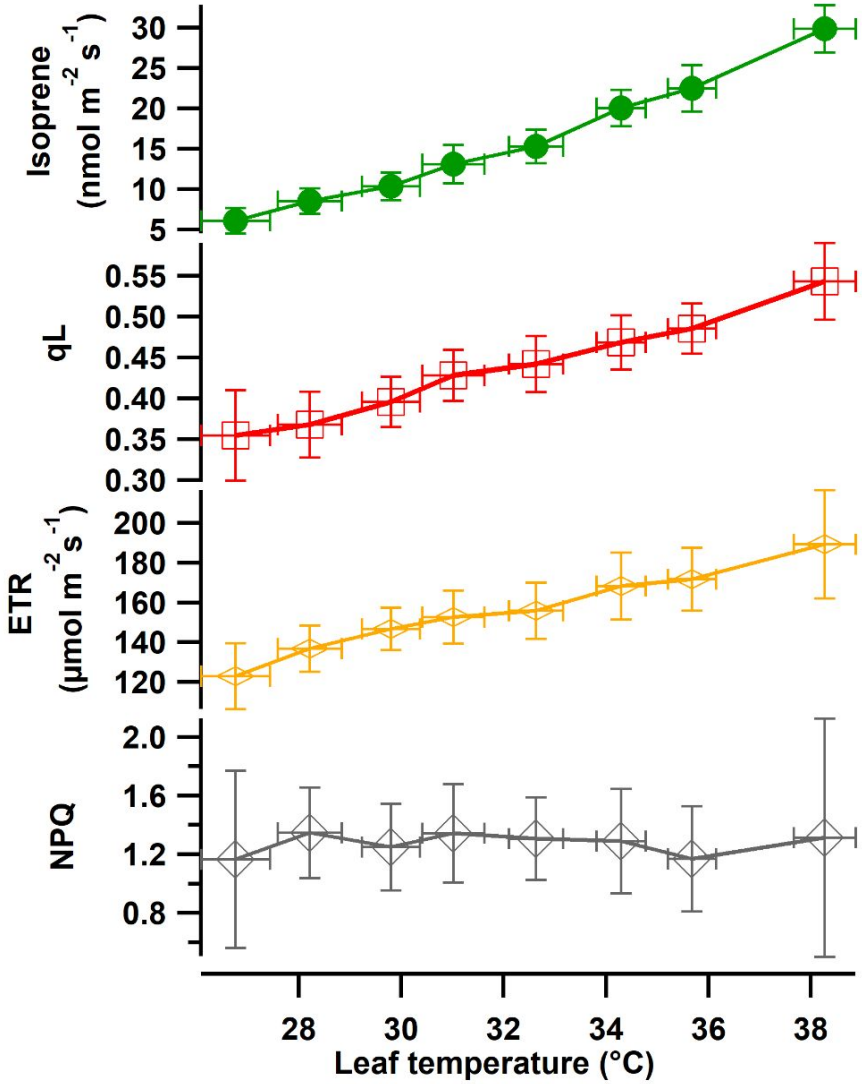

Figure 2: Mean *V. guianensis* leaf temperature responses of light-dependent photosynthetic parameters including electron transfer rate (ETR), oxidation state of Q_A (q_L), and non-photochemical quenching (NPQ) together with leaf isoprene emissions. Data shown are the mean of 23 temperature response curves collected with error bars representing ± 2 standard deviation.

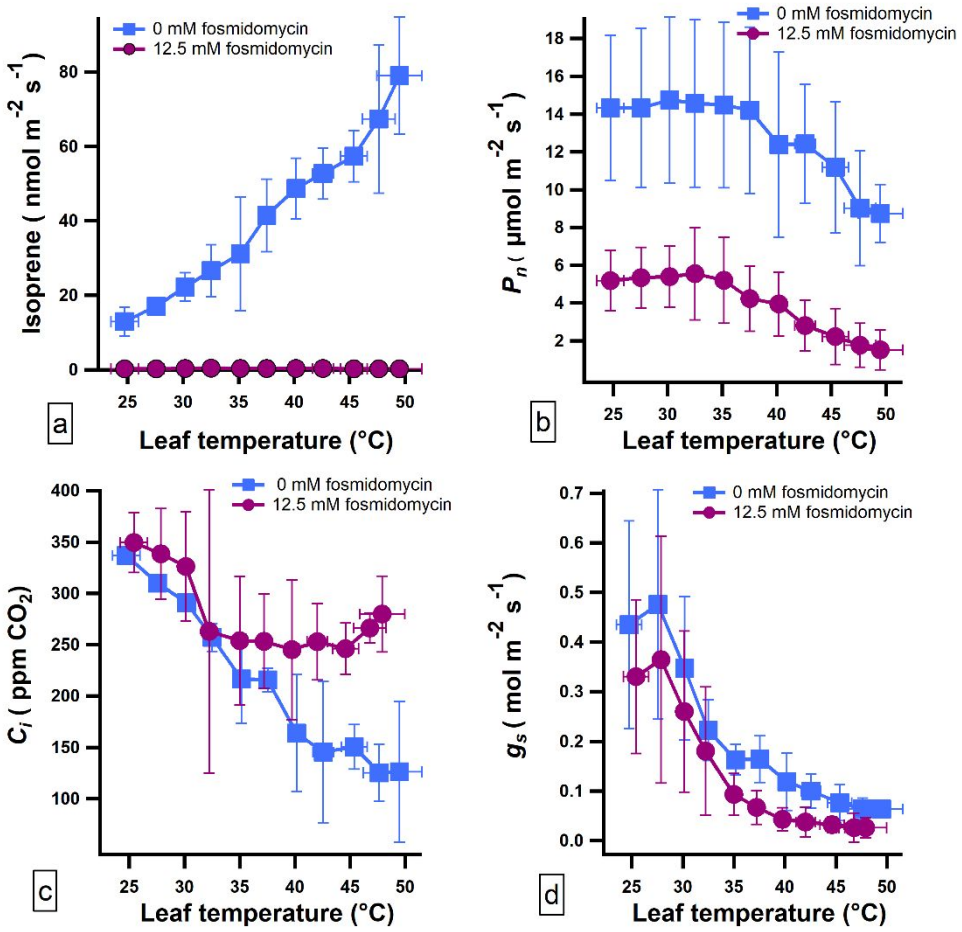

Figure 3: Mean *V. guianensis* leaf temperature responses after 1 hour of branch feeding with 0 mM (blue curves with squares) and 12.5 mM (purple curves with dots) of the isoprenoid pathway inhibitor fosmidomycin showing (**a**) isoprene emissions, (**b**) net photosynthesis, P_n, (**c**) intercellular CO_2 concentration, C_i, (**d**) stomatal conductance, g_s. Data shown are the mean of 3-4 temperature response curves (1 curve per leaf) with error bars representing ± 2 standard deviation.

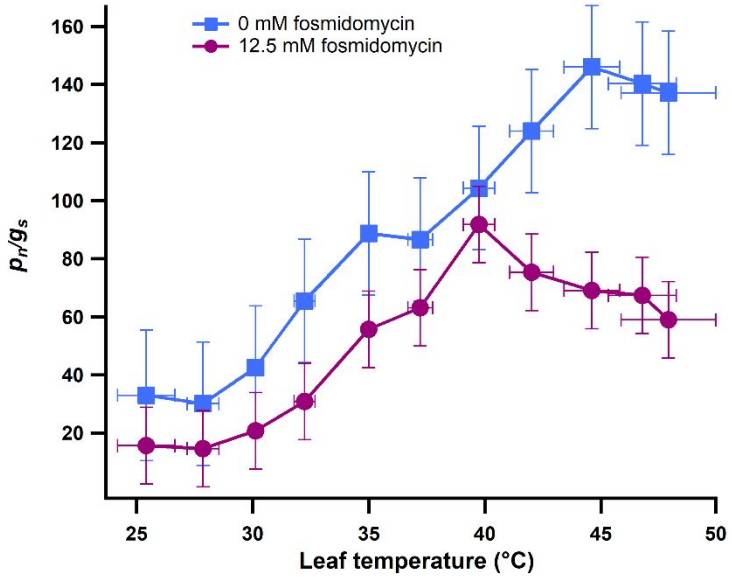

Figure 4: Mean *V. guianensis* leaf temperature responses after 1 hour of branch feeding with 0 mM (blue curves with squares) and 12.5 mM (purple curves with dots) of the isoprenoid pathway inhibitor fosmidomycin showing net photosynthesis normalized to stomatal conductance, P_n/g_s. Data shown are the mean of 3-4 temperature response curves (1 curve per leaf) with error bars representing ± 2 standard deviation.

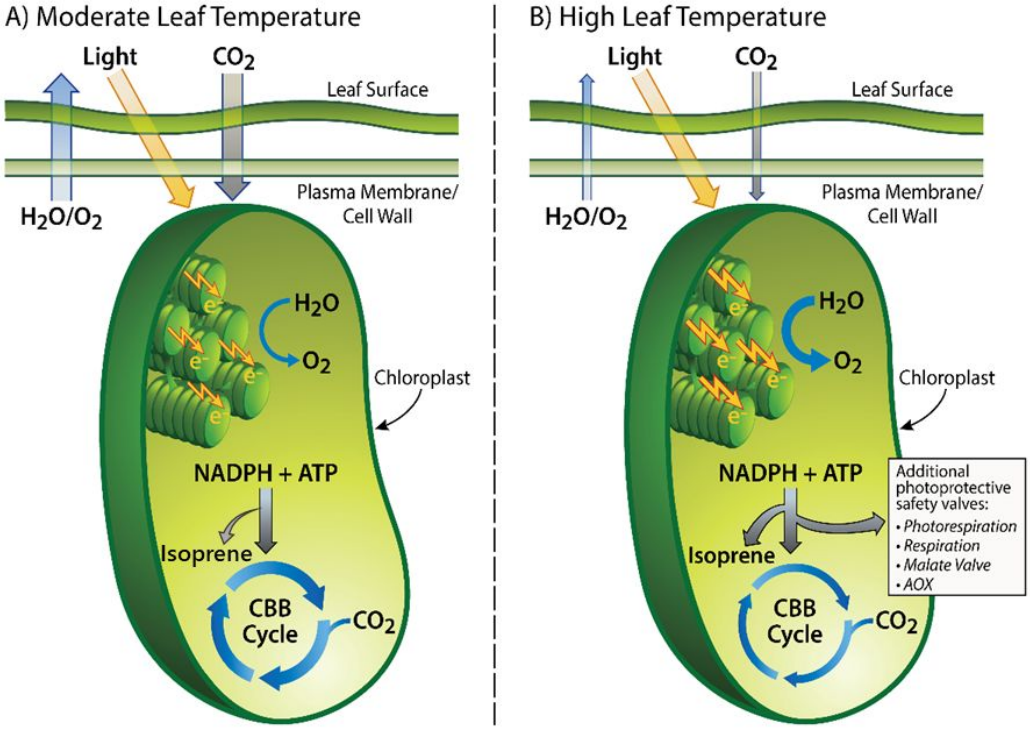

Figure 5: Proposed biochemical model of the acclimation to high temperature stress through the consumption of photosynthetic energy (ATP) and reducing equivalents (NADPH) through the activation of the isoprenoid pathway together in parallel with other coupled biochemical pathways (adapted from Voss *et al*., 2013 and Morfopoulos *et al*., 2014). O_2: oxygen; CO_2: carbon dioxide; H_2O: water; ATP: adenosine triphosphate; NADPH: Nicotinamide-Adenine-Dinucleotide-Phosphate; AOX: alternative oxidases of mitochondria.

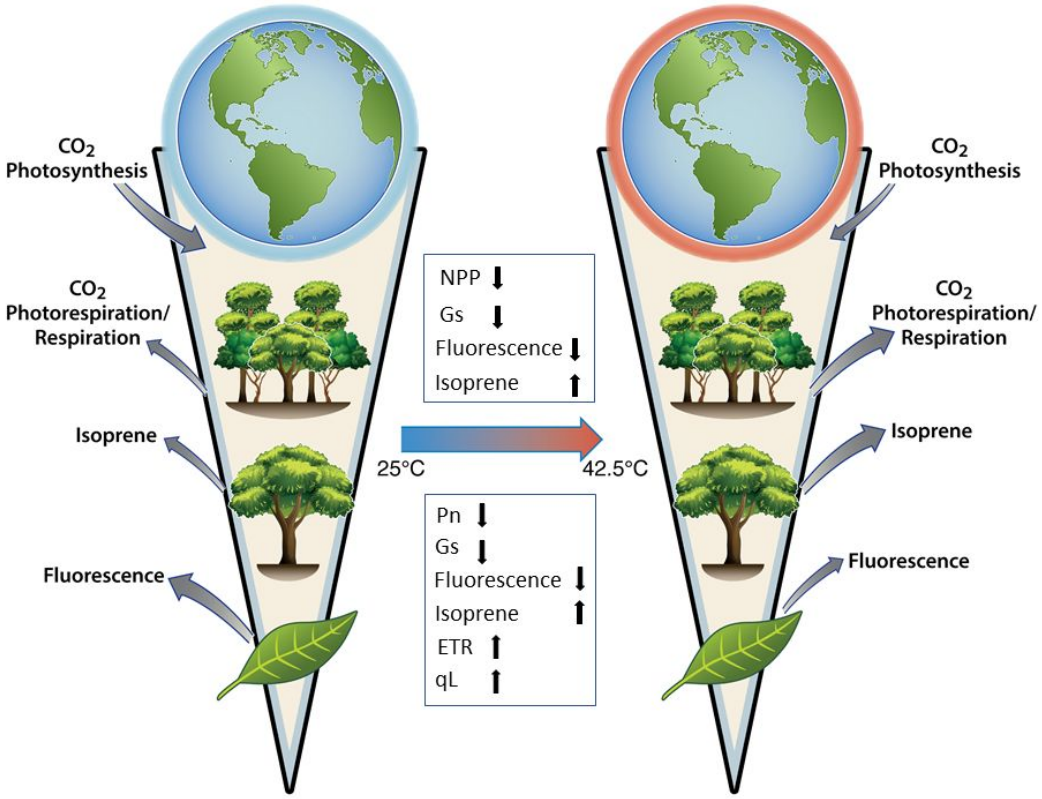

Figure 6 (Graphical Abstract): Graphical representation the influence of proposed surface temperature impacts on plant physiological processes influencing terrestrial ecosystem carbon cycling from leaf to global scales. NPP: Net Primary Productivity, Gs: Stomatal Conductance, ETR: Electron Transport Rate, qL: Fraction of PSII centers that are oxidized, CO_2: carbon dioxide.

	P_n	g_s	Fv'/Fm'	NPQ	ETR	Isoprene	C_i	qL
P_n	1	0.73	0.57	-0.38	-0.75	-0.68	0.63	-0.65
g_s	0.73	1	0.62	-0.05	-0.97	-0.97	0.97	-0.97
Fv'/Fm'	0.57	0.62	1	-0.33	-0.67	-0.53	0.46	-0.60
NPQ	-0.38	-0.05	-0.33	1	0.19	0.09	0.13	0.13
ETR	-0.75	-0.97	-0.67	0.19	1	0.98	-0.93	0.99
Isoprene	-0.69	-0.97	-0.53	0.09	0.98	1	-0.97	0.99
C_i	0.63	0.97	0.46	0.13	-0.93	-0.97	1	-0.95
qL	-0.65	-0.97	-0.60	0.13	0.99	0.99	-0.95	1

915 **Table 1**: Correlation (*r*) derived between the gas exchange (P_n, g_s, and isoprene emissions) and
916 light-independent photosynthetic variables shown in **Figs. 1-2**.

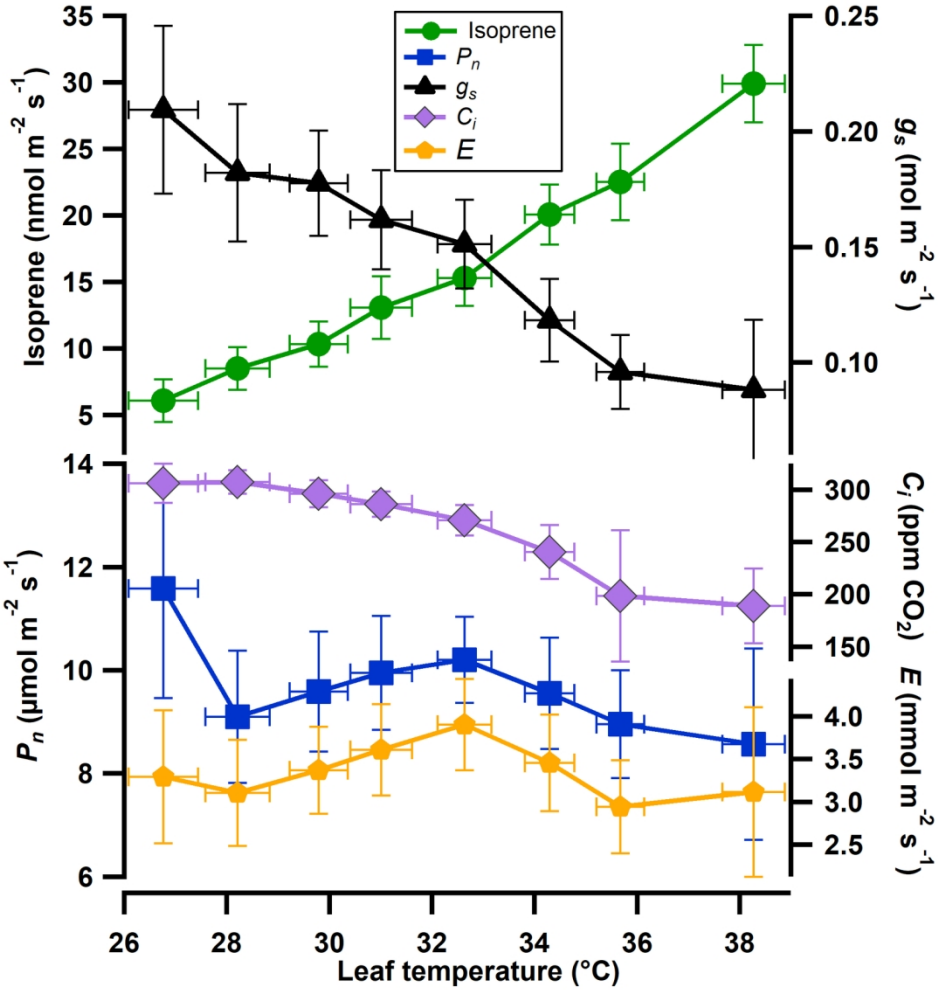

Figure 1: Mean response of net photosynthesis (Pn), stomatal conductance (gs), internal carbon (Ci), transpiration (E), and isoprene emissions to an increase in leaf temperature in V. guianensis. Data shown are the mean of 23 temperature response curves collected with error bars representing ± 2 standard deviation.

152x153mm (300 x 300 DPI)

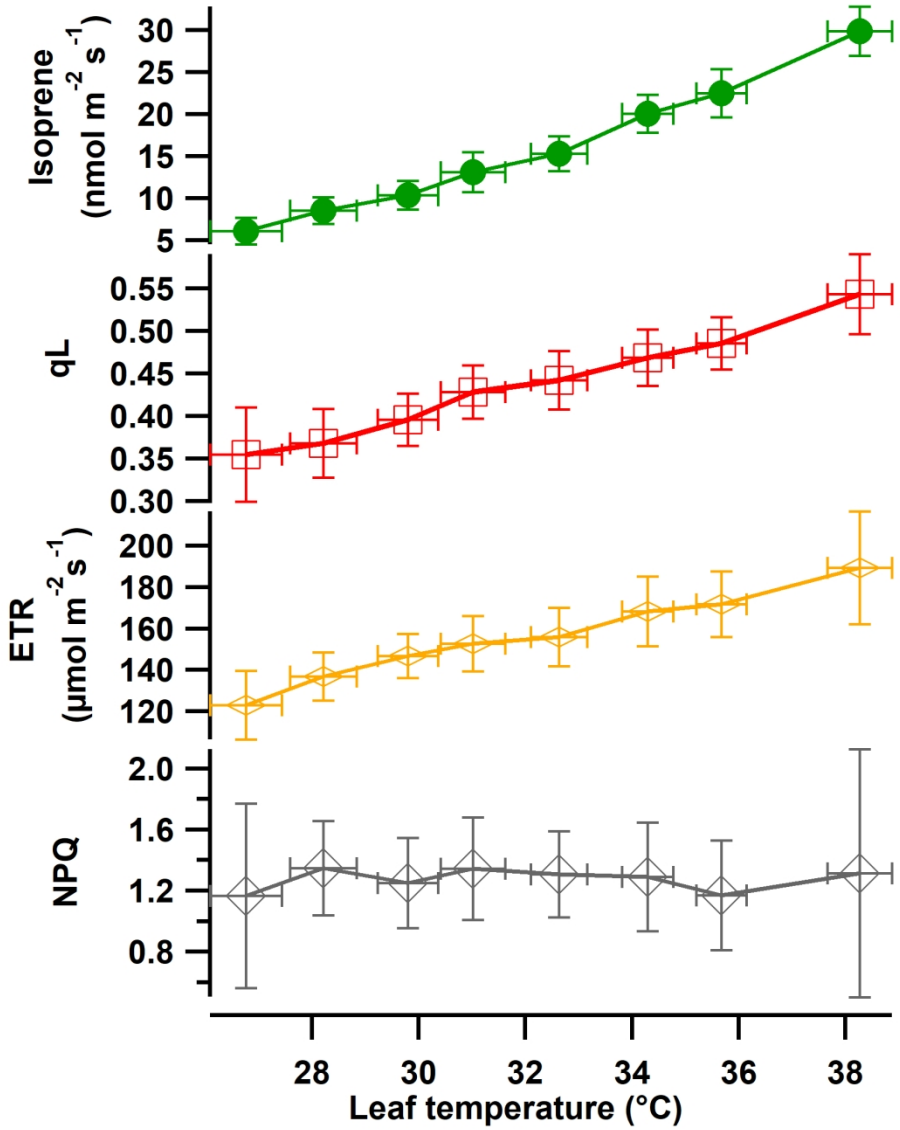

Figure 2: Mean *V. guianensis* leaf temperature responses of light-dependent photosynthetic parameters including electron transfer rate (ETR), oxidation state of QA (q_L), and non- photochemical quenching (NPQ) together with leaf isoprene emissions. Data shown are the mean of 23 temperature response curves collected with error bars representing ± 2 standard deviation.

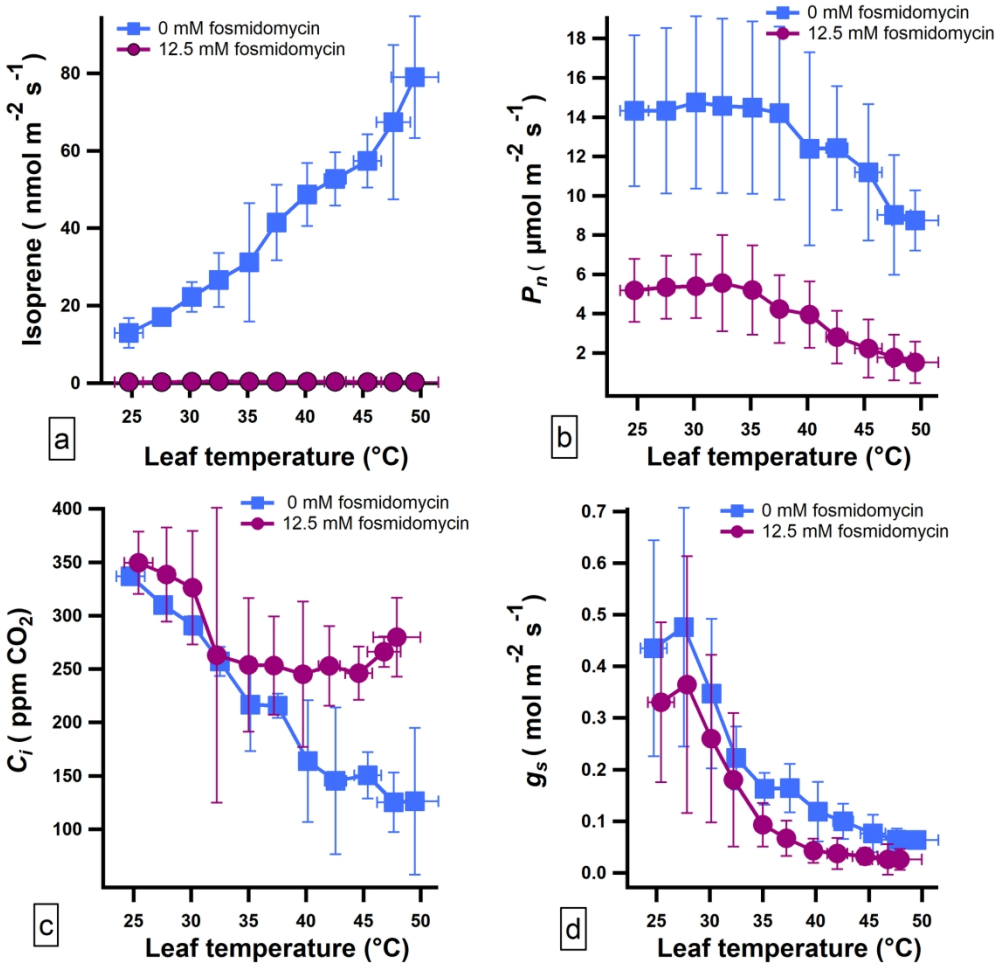

Figure 3: Mean V. guianensis leaf temperature responses after 1 hour of branch feeding with 0 mM (blue curves with squares) and 12.5 mM (purple curves with dots) of the isoprenoid pathway inhibitor fosmidomycin showing (a) isoprene emissions, (b) net photosynthesis, Pn, (c) intercellular CO2 concentration, Ci, (d) stomatal conductance, gs. Data shown are the mean of 3-4 temperature response curves (1 curve per leaf) with error bars representing ± 2 standard deviation.

191x187mm (300 x 300 DPI)

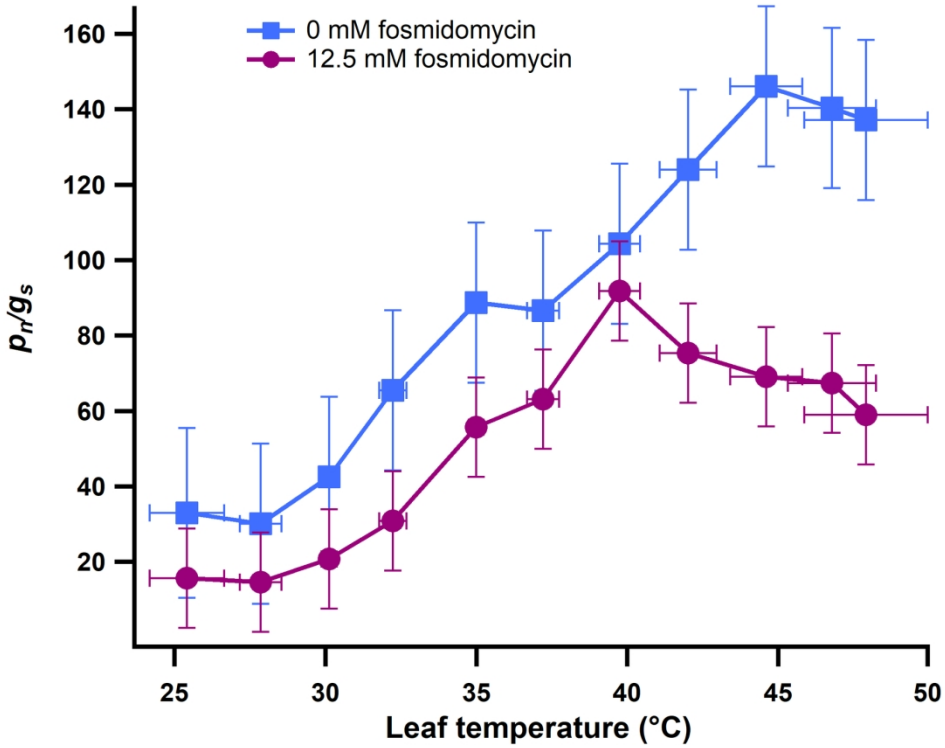

Figure 4: Mean V. guianensis leaf temperature responses after 1 hour of branch feeding with 0 mM (blue curves with squares) and 12.5 mM (purple curves with dots) of the isoprenoid pathway inhibitor fosmidomycin showing net photosynthesis normalized to stomatal conductance, Pn/gs. Data shown are the mean of 3-4 temperature response curves (1 curve per leaf) with error bars representing ± 2 standard deviation.

165x127mm (300 x 300 DPI)

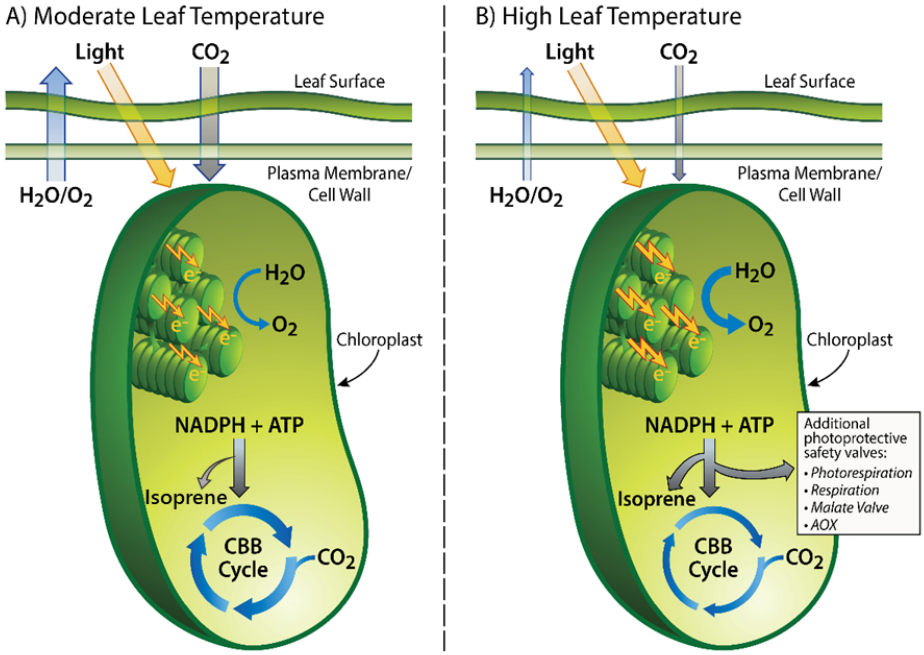

Figure 5: Proposed biochemical model of the acclimation to high temperature stress through the consumption of photosynthetic energy (ATP) and reducing equivalents (NADPH) through the activation of the isoprenoid pathway together in parallel with other coupled biochemical pathways (adapted from Voss *et al.*, 2013 and Morfopoulos *et al.*, 2014). O_2: oxygen; CO_2: carbon dioxide; H_2O: water; ATP: adenosine triphosphate; NADPH: Nicotinamide-Adenine-Dinucleotide-Phosphate; AOX: alternative oxidases of mitochondria.

254x190mm (96 x 96 DPI)